Karlsruhe Institute of Technology

# Overview on HLM-related Activities for Fusion and Nuclear Applications at KIT

INSTITUTE FOR APPLIED MATERIALS – MATERIAL PROCESS TECHNOLOGY | CORROSION DEPARTMENT

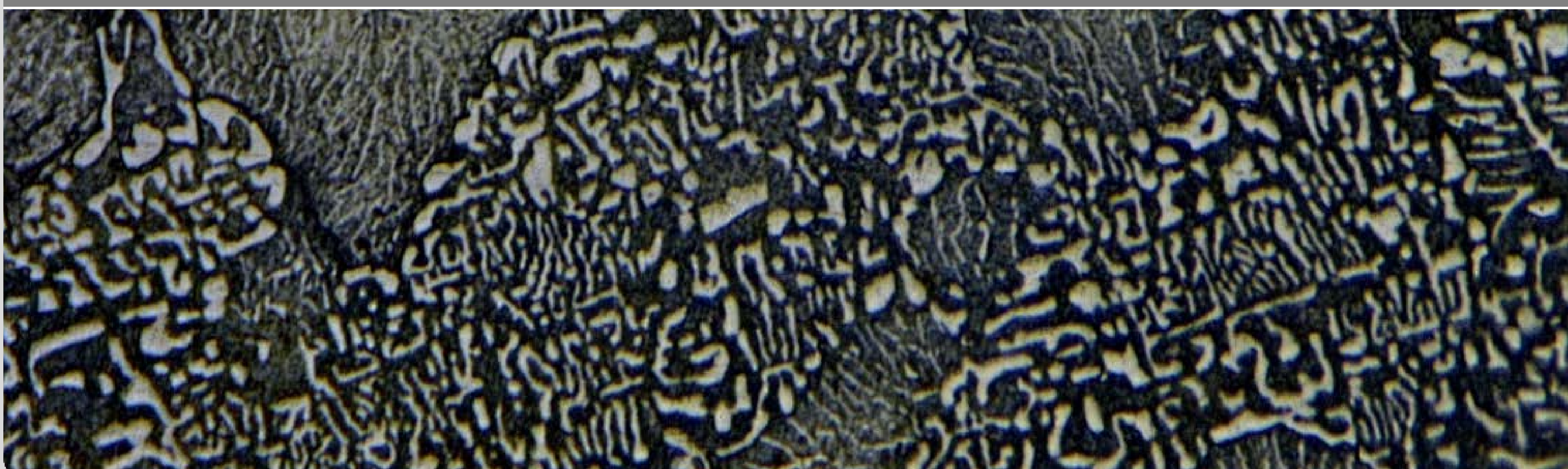

# Bird‘s eye view of KIT campus north (former FZK)

# Outline

1) Application of heavy liquid metals for Fusion and Nuclear energy production

2) Corrosion testing and corrosion modeling of EUROFER steel in flowing Pb-15.7Li for fusion application

3) Development of advanced processes for Al-based anti-corrosion and T-permeation barriers for HLM environments

4) Non-metal chemistry of heavy liquid metal corrosion of iron-based structural materials at KIT

5) Creep-rupture testing of ODS-steels in Pb at 650°C

6) Conclusions

# Application of Heavy Liquid Metals for Fusion and Nuclear Energy Production

**The use of eutectic Pb-15.7Li alloy for the European HCLL blanket concept**

**Thermo-nuclear power reactor**

D + T $\Rightarrow$ n (14.1 MeV) + He (3.52 MeV)

**Tritium is generated from Li**

$^{6}$Li + n $\Rightarrow$ T + He + 4.8 MeV
$^{7}$Li + n $\Rightarrow$ T + He + n' - 2.87 MeV

**Eutectic Pb-15.7Li**
0.65 mass% Li, $T_m$ = 235°C

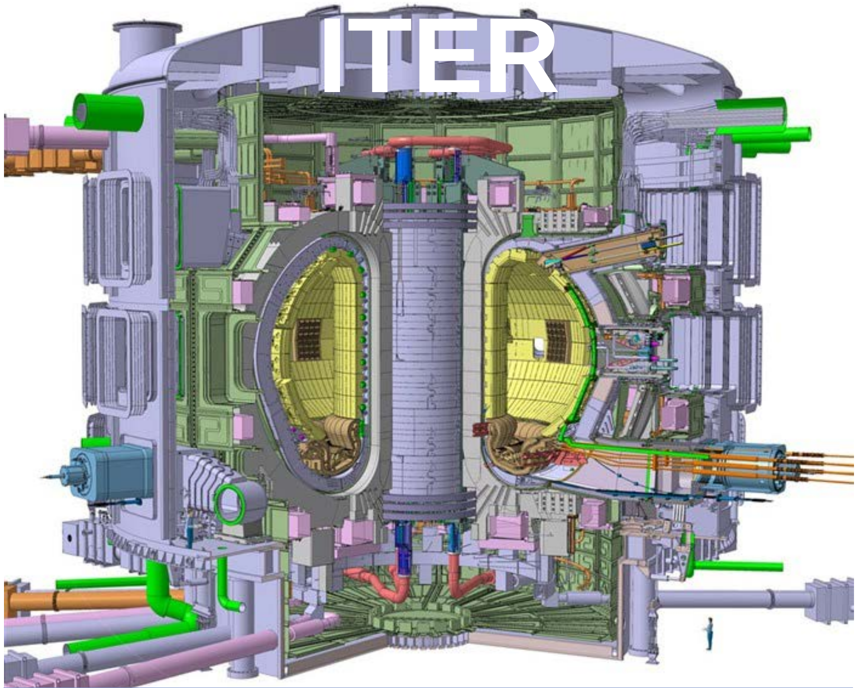


HCLL = Helium-Cooled Lithium-Lead

# The HCLL (He-PbLi) TBM (and DEMO) Blanket

| DEMO HCLL MAIN FEATURES |
|---|
| 2m x 2m modules |
| RAFM steel (e.g. EUROFER) |
| He (8 MPa, 300-500°C) |
| Liquid Pb-15.7Li (eutectic) as breeder and multiplier |
| PbLi slowly re-circulating (10/50 rec/day) |
| 90% $^{6}$Li in PbLi<br><br>Pb-Li velocities in breeding unit ~ 1 cm/s range |
| TBR = ≤1.15 with 550mm Breeder radial depth |
| Lifetime 7.5 MWy/m$^2$ |

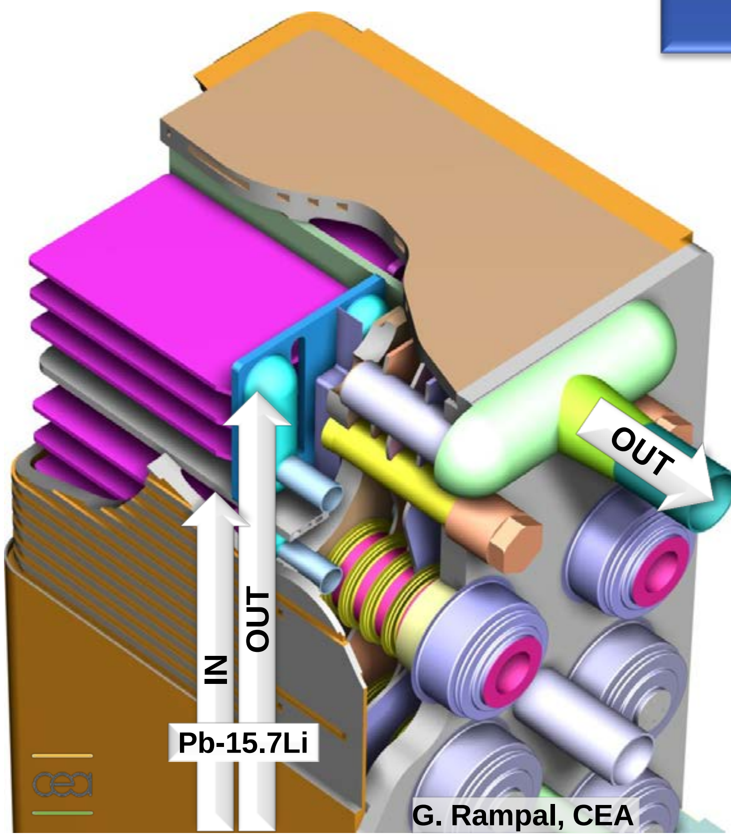


**Corrosion of cooling and stiffening plates and permeation of tritium from PbLi into He gas**

**PbLi flow velocity ~ 1 cm/s**

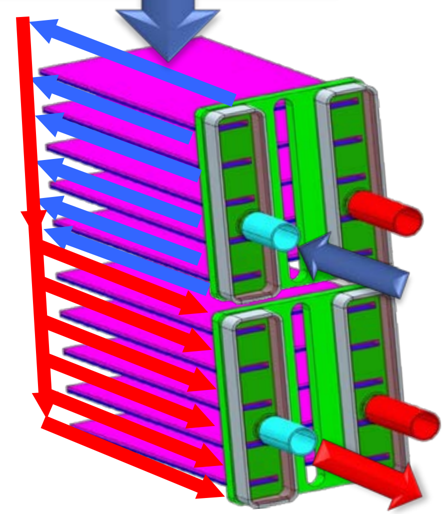

# Lead-cooled Nuclear Reactors/Systems

Karlsruhe Institute of Technology

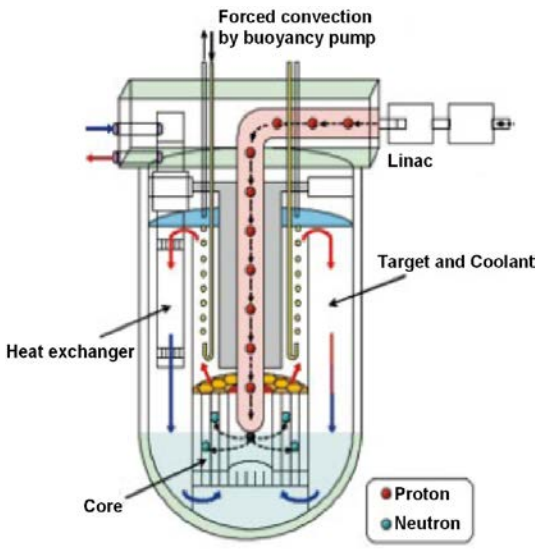


## Accelerator Driven (Subcritical) System

- Transmutation of long-lived radioactive isotopes in nuclear waste
- Power generation
- Liquid lead (Pb) or lead-bismuth eutectic (LBE) as spallation target and primary coolant
- Maximum temperature, typically
  - 450 – 500°C for regular operation
  - Periodically 550°C (according to plant design)

## Lead-Cooled Fast Reactor

- One of the concepts for the 4th generation of nuclear power plants (Gen IV)
- In the long-term, Pb as primary coolant at maximum ca. 800°C
- Short- to mid-term: Pb- or LBE-cooled at 600 – 650°C

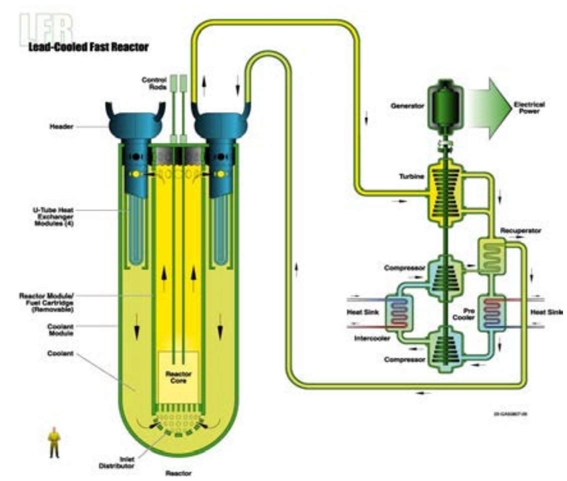

# Some Specific Properties of (Heavy) Liquid Metals

| | | UNIT | $Pb^{45}B^{i55}$ | LITHIUM | WATER |
|---|---|---|---|---|---|
| **Melting Point at 0.1 MPa** | | [°C] | 125 | 180.5 | 0 |
| **Boiling Point at 0.1 MPa** | | [°C] | 2516 | 1317 | 100 |
| | | | | | |
| | | | **300°C** | **300°C** | **25°C** |
| **Density** | $\rho$ | [kg/m$^3$] | 10325 | 505 | 1000 |
| **Heat Capacity** | $c_\rho$ | [J/(kgK)] | 146.33 | 4279 | 4180 |
| **Kinematic Viscosity** | $\nu$ | [m2/s] $\cdot 10^{-7}$ | 1.754 | 9 | 9.1 |
| **Heat Conductivity** | $\lambda$ | [W/(m K)] | 12.68 | 29.2 | 0.6 |
| **Electric Conductivity** | $\sigma_{el}$ | [A/(V m)] $\cdot 10^5$ | 8.428 | 33.5 | $2 \cdot 10^{-4}$ (tap) |
| **Thermal Expansion Coefficient** | $\alpha$ | [K$^{-1}$] $\cdot 10^{-3}$ | 6.7 | 43.6 | 6 |
| **Surface Tension** | $\sigma$ | [N/m] $\cdot 10^{-3}$ | 410 | 421 | 52 (tap) |

# Phase Diagram Lead – Bismuth (Pb-Bi)

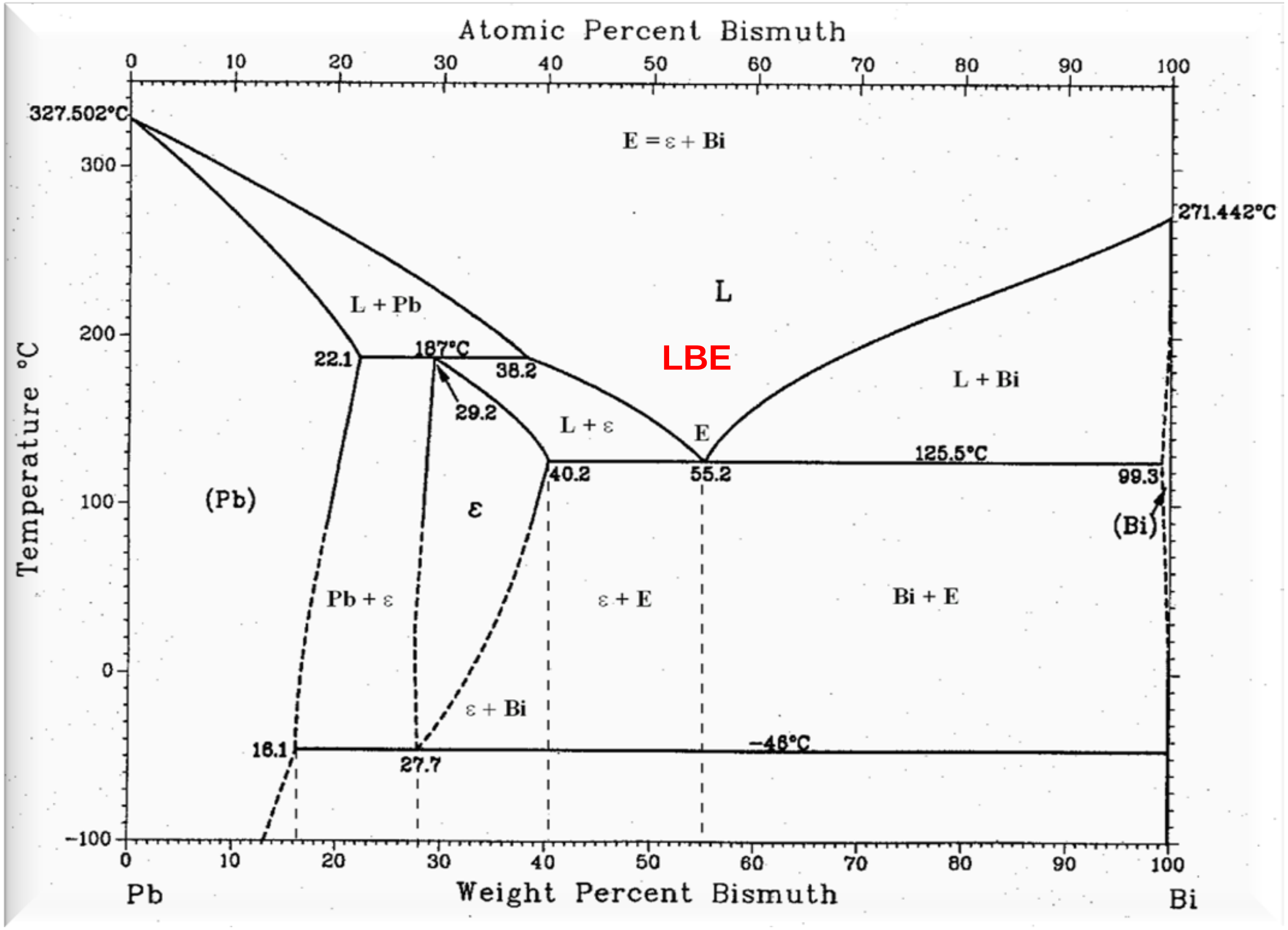


LBE = Lead-Bismuth Eutectic

# Phase Diagram Lead – Lithium (Pb-Li)

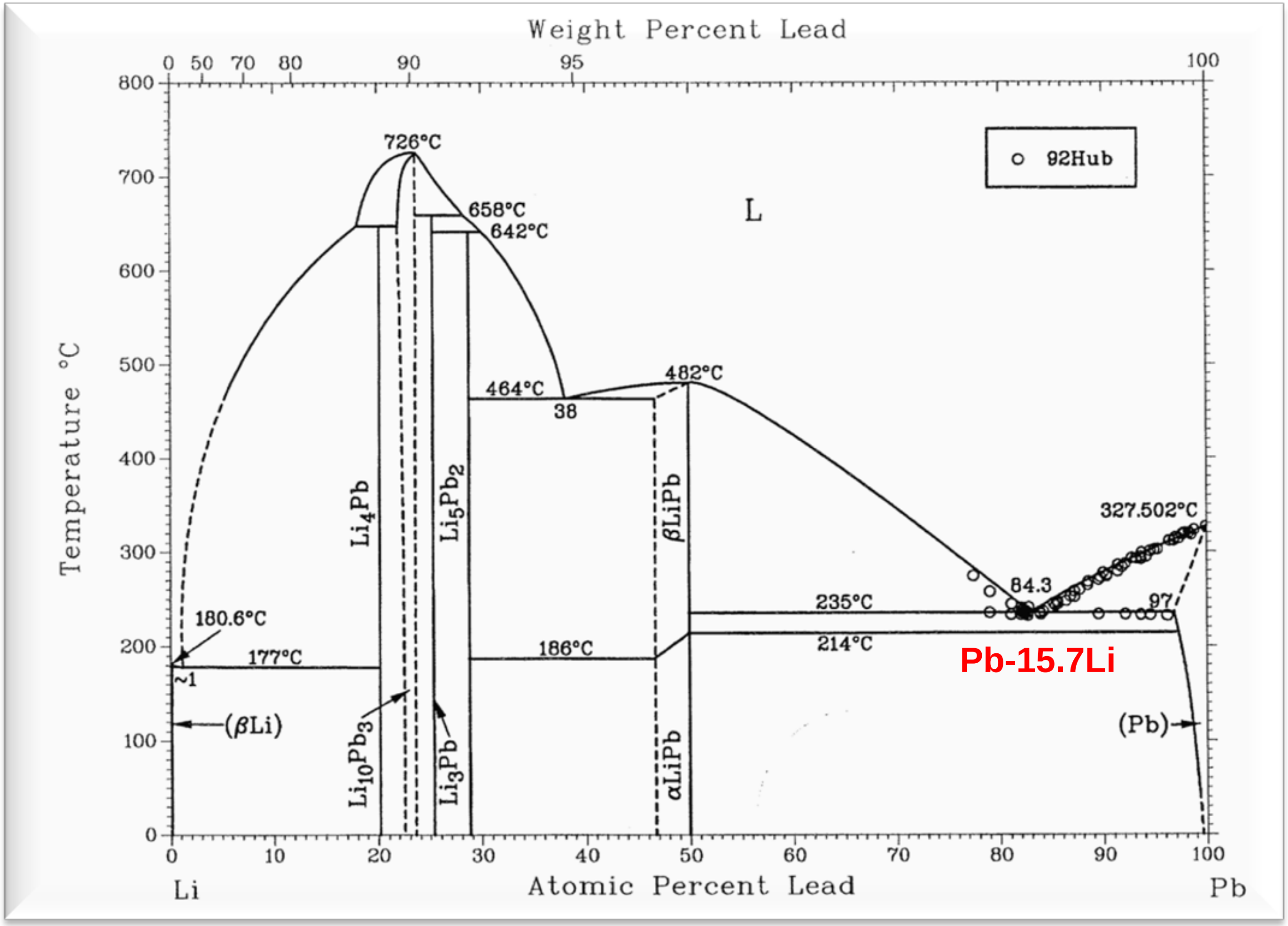

# Oxygen Potentials of Metal/Metal-oxides, relevant for the Stability of Structural Materials in

## Pb, LBE

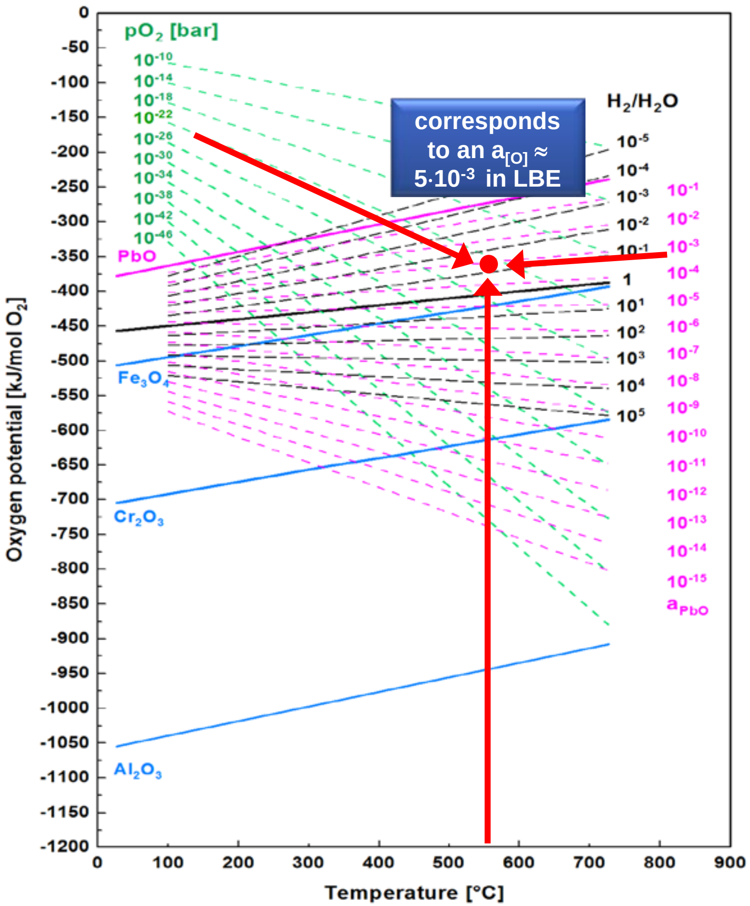


## Pb-15.7 Li

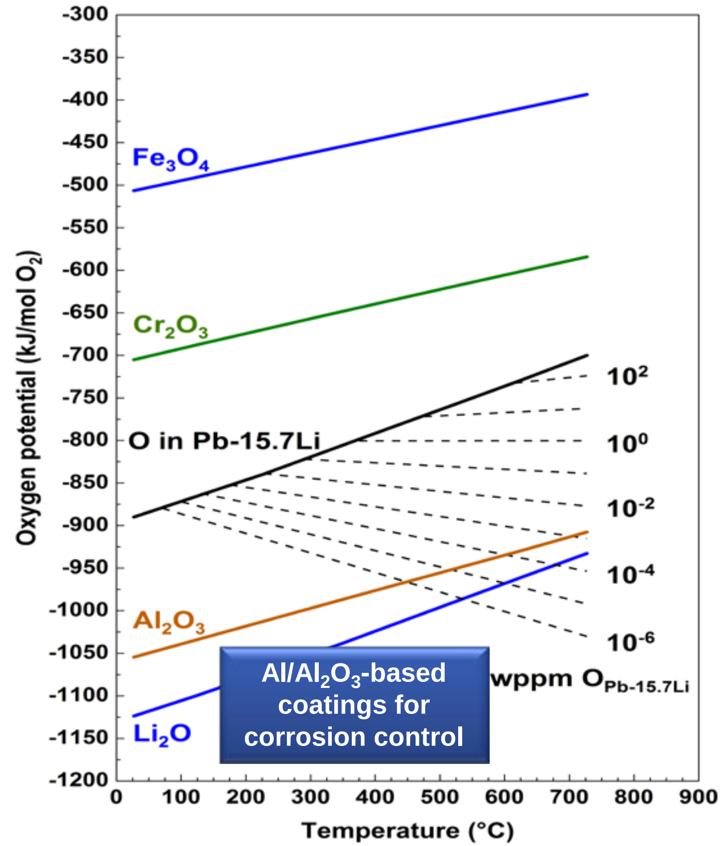

# Corrosion testing and modeling of EUROFER steel in flowing Pb-15.7Li for fusion application

**Outline**

- Existing data at KIT
  - Formation of precipitates
- Relevance of flow rate for HCLL-TBM
- Modeling of corrosion/precipitation with MATLIM code
  - Calculations with MATLIM code and comparison with experimental data
- Corrosion test results
  - Campaign at 10 cm/s

# Corrosion testing and corrosion modeling of EUROFER steel in flowing Pb-15.7Li

Karlsruhe Institute of Technology

## Introduction

Reduced activation ferritic-martensitic steels, e.g. EUROFER, are considered as structural materials for TBMs in ITER

EUROFER is in direct contact with the liquid breeder Pb-15.7Li in the HCLL blanket concept

For the design of PbLi-operated TBMs and for future blankets in DEMO, a reliable and safe long-term operation must be guaranteed

This means for R&D respectively for experimental data evaluation:

- Long-term corrosion data at relevant conditions (T, v) must be available
- The precipitation behavior of Fe-(Cr) particles in PbLi must be understood
- .... and the development of modeling tool has to be carried out

# Pb-15.7Li corrosion testing in PICOLO loop

**PICOLO is a major loop for Pb-15.7 Li corrosion testing in frame of TBM consortium**

Karlsruhe Institute of Technology

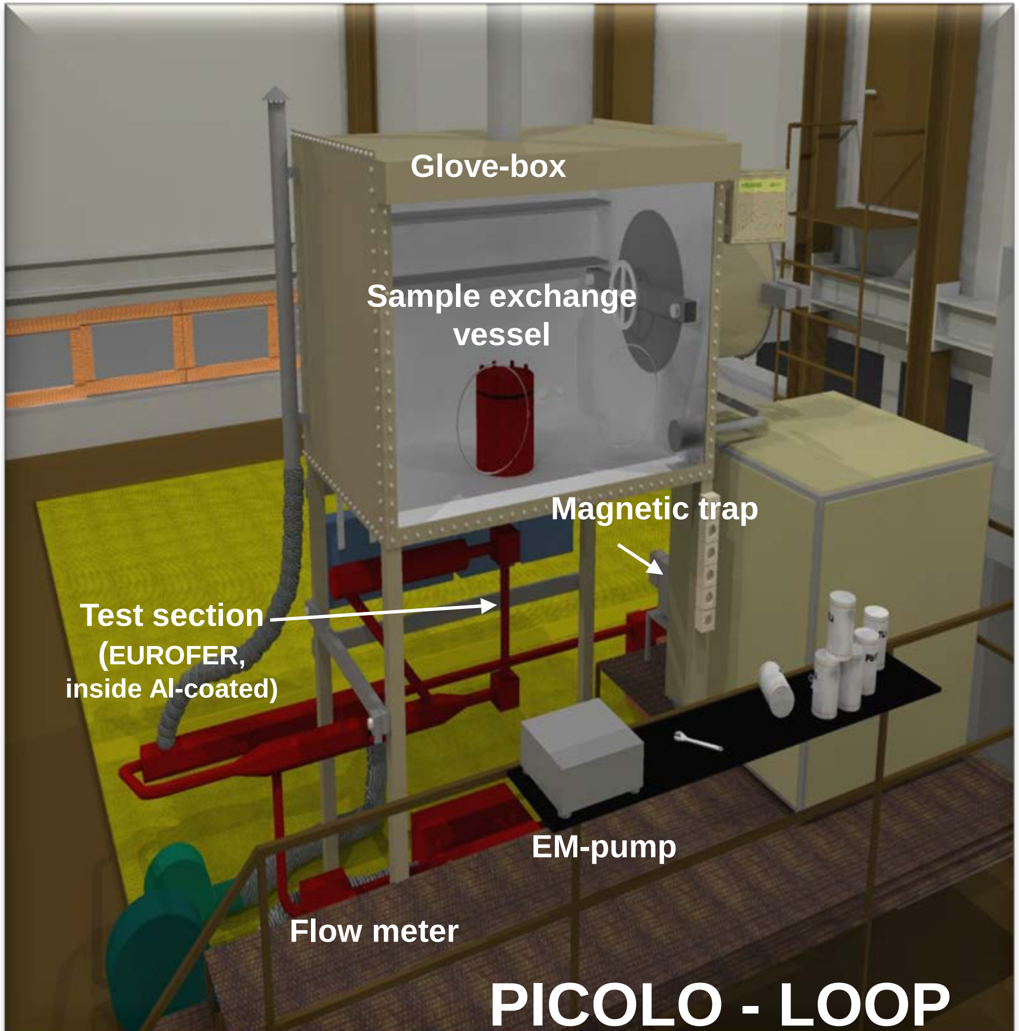


**Parameters of Pb-15.7Li Loop PICOLO**

| | |
|---|---|
| Test temperature: | 480-550°C |
| $T_{max}$ in test section: | 550°C |
| $T_{low}$ at EM-pump: | 350°C |
| Pb-15.7Li volume: | 20 litres |
| Flow velocity range: | 0.01 - 1 m/s |
| Test velocity up to 2007: | 0.22 m/s |
| Loop materials: | |
| Cold legs: | 18 12 CrNi steel |
| Hot legs: | 10 % Cr steel |
| Total loop operation: | |
| at 480°C | > 125,000 h |
| at 550°C | > 15,000 h |

**Test conditions since 2008**

| | |
|---|---|
| Pb-15.7Li velocity | 0.1 m/s |

Compromise to laminar/turbulent flow regimes, data for modeling and TBM requirements

# Experimental


Diameter: 8 mm
Length: 35 mm

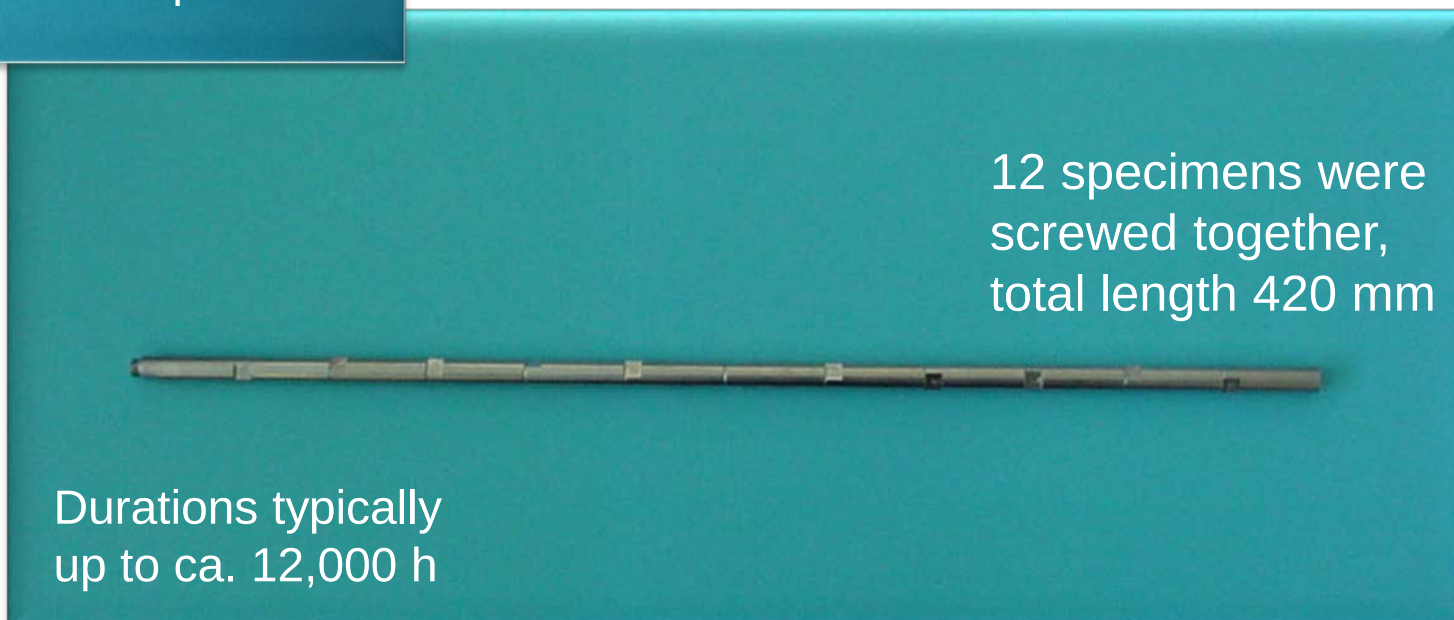

# Experience from corrosion testing in PICOLO loop

Karlsruhe Institute of Technology

**Precipitation and transport behavior of corrosion products**

- Only rudimentarily data on transportation effects of corrosion products and their precipitation behavior are available.
- Only some small sections of PICOLO loop are analysed.
- But high risk was detected for loop blockages due to precipitations.
- New testing campaigns are extended to smaller flow rates towards mixed and laminar conditions with more TBM relevance.

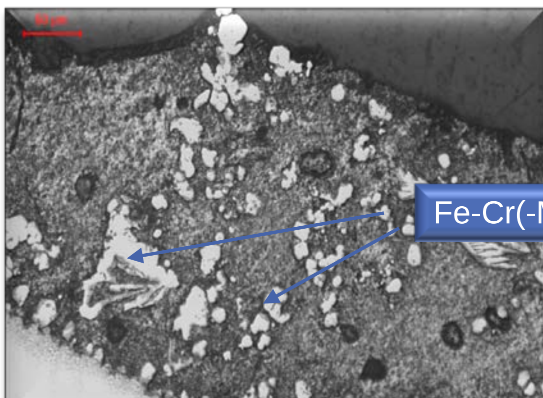

Formed and transported precipitations

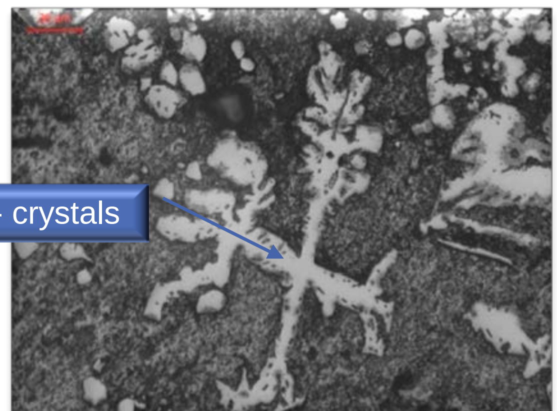
Precipitations in adherent Pb-15.7Li scale

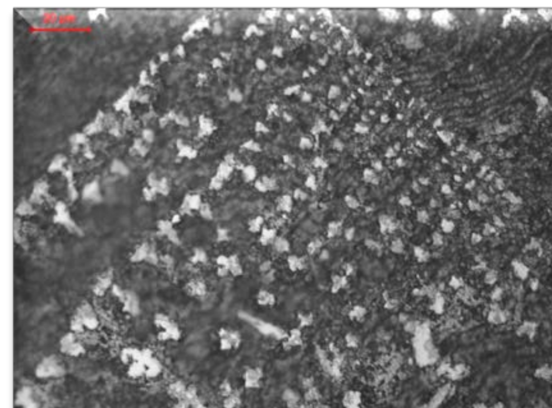
Precipitations in the centre of the magnetic trap, parallel to field lines

# TBM test conditions concerning corrosion

**Figures of merit for TBM/DEMO derived from PICOLO tests and modeling by MATLIM**

| Geometry of test section Picolo | Geometry of TBM |
|---|---|
| 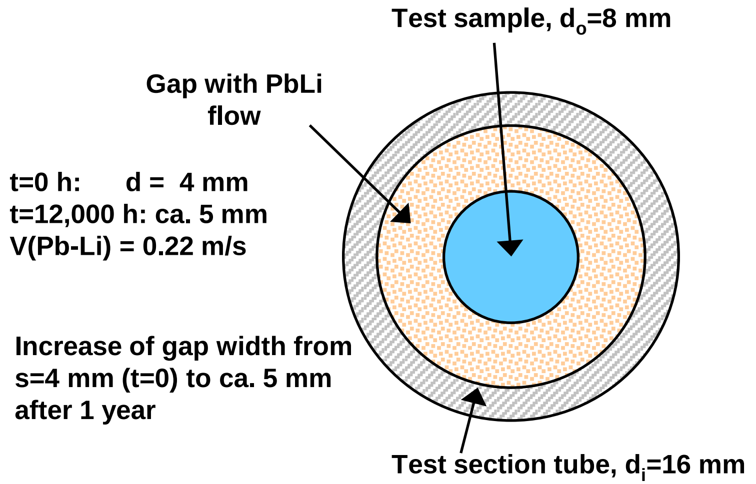 | 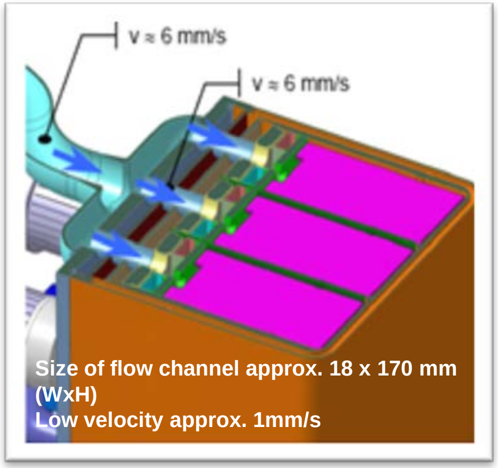 |





**The flow in pipes is laminar up to a Reynolds number of ca. 2,300 and it becomes fully turbulent at a Reynolds number of e.g. 10,000.**

| Hydraulic diameter Picolo | Hydraulic diameter TBM |
|---|---|
| $d_{hyd}$ = 4A/U = d − d0 = 2s<br>$d_{hyd}$ = 0.8 cm | dhyd = 4A/U = 4 (WxH) /2 (W+H)<br>dhyd = 3.25 cm |

# TBM Test Conditions Concerning Corrosion

**Envisaged Reynolds number for TBM Re = some 100 in accordance with MHD calculations of L. Bühler, KIT**

| | PICOLO 22 cm/s | PICOLO 10 cm/s | PICOLO 1 cm/s | TBM 0.1 cm/s |
|---|---|---|---|---|
| Reynolds $Re= u_{fl}\ d_{hyd}/\nu_{fl}$ | 22 * 0.8 / 0.105 * $10^{-2}$ = (17.6 /10.5) *$10^4$ = 16,800 | 10 * 0.8 / 0.105 * $10^{-2}$ = (8 /10.5) *$10^4$ = 7,620 | 1 * 0.8 / 0.105 * $10^{-2}$ = (0.8 /10.5) *$10^4$ = 762 | 0.1 * 3.25 / 0.105 * $10^{-2}$ = 0.325/10.5 * $10^4$ = 310 100<Re<1000 |
| | turbulent | Main part turbulent | laminar | laminar |
| Schmidt $Sc = \nu_{fl} / D$ | 0.105 * $10^{-2}$ / 1,185 * $10^{-6}$ = 860 | = 860 | = 860 | = 860 |
| Sherwood number for laminar flow in Picolo is assumed to be 3.66 “Inlet” corrections have to consider the Graetz number : G = Re Pr d / l | | | | |

# TBM Test Conditions Concerning Corrosion

Karlsruhe Institute of Technology

**Selection of corrosion relevant parameters for TBM simulation in future PICOLO testing**

- In order to get a Re number of some 100, flow rate in TBMs should be near 1.0 mm/s.
- PICOLO testing at 1 cm/s would fulfil laminar flow quite well below Re = 2500 but with a Re = 760.
- Nevertheless, testing at 0.1 cm/s (1 mm/s) may form type of pipe flows and back flows which might not result in homogeneous flow conditions.

# Analyses of ITER-TBM tests vs. state-of-the-art

**Key issues towards ITER-TBM testing and modeling**

**Generally:**
Quantitative corrosion-testing in dynamic lead-lithium eutectic at TBM- and DEMO-relevant conditions

**Key issues to be addressed:**

- Channel configuration different to all loop tests
- Corrosion in TBM geometries and flow velocity profiles "unknown"
- Influence of magnetic field on corrosion
- Retention of precipitates inside of TBM
- Effects of impurities in Pb-15.7Li on corrosion/precipitation
- Composition changes of Pb-15.7Li during operation
- $H_2$-effects on corrosion and precipitation behavior
- Effective purification system
- Stability of barriers under TBM conditions
- Validation of modeling tools and codes
- Risk assessment for system blocking

➔ **Definition of activities for development towards DEMO**

# Modeling of Corrosion/Precipitations with MATLIM code

Karlsruhe Institute of Technology

**Necessary elements for the calculation of dissolution and precipitation rates**

- Mass flux $j_i$ of the solute $i$ from the channel wall into the bulk of the fluid with $c_i^w$ as the concentration of the solute at the wall and $c_i^b$ in the bulk of the fluid:

$$j_i = K_i^{fl} \cdot (c_i^w - c_i^b)$$

Flux direction:

wall $\begin{array}{c} c_i^w > c_i^b \\ \longrightarrow \\ \longleftarrow \\ c_i^w < c_i^b \end{array}$ fluid

- Mass transfer coefficient $K_i^{fl}$, determined by the Sherwood number Sh, the diffusivity of the solute $i$ in the liquid metal $D_i$ and the hydraulic diameter $d_{hyd}$:

$$K_i^{fl} = \frac{D_i}{d_{hyd}} \cdot Sh$$

- Dependence of the Sherwood number on the Reynolds number and on the Schmidt number under forced flow conditions:

$$Sh = a \cdot \mathrm{Re}^{\alpha} \cdot Sc^{\beta}$$ with $$\mathrm{Re} = \frac{u_{fl} \cdot d_{hyd}}{\upsilon_{fl}}$$ and $$Sc = \frac{\upsilon_{fl}}{D_i}$$

*a*, $\alpha$, $\beta$ are to be determined experimentally depending on the flow regime

$u_{fl}$: flow velocity

$v_{fl}$: kinematic fluid viscosity

- Correlation of the mass transfer coefficient under turbulent flow acc. to Silverman:

$$K_{Silv} = 0.0177 \cdot u_{fl}^{0.875} \cdot D_{Fe}^{0.704} / (d_{hyd}^{0.125} \cdot \upsilon_{fl}^{0.567})$$

# Modeling of Corrosion/Precipitations with MATLIM code

**Axial Distributions of the Flow Velocity and Hydraulic Diameter in PICOLO Loop at 550°C (q=120 l/h)**

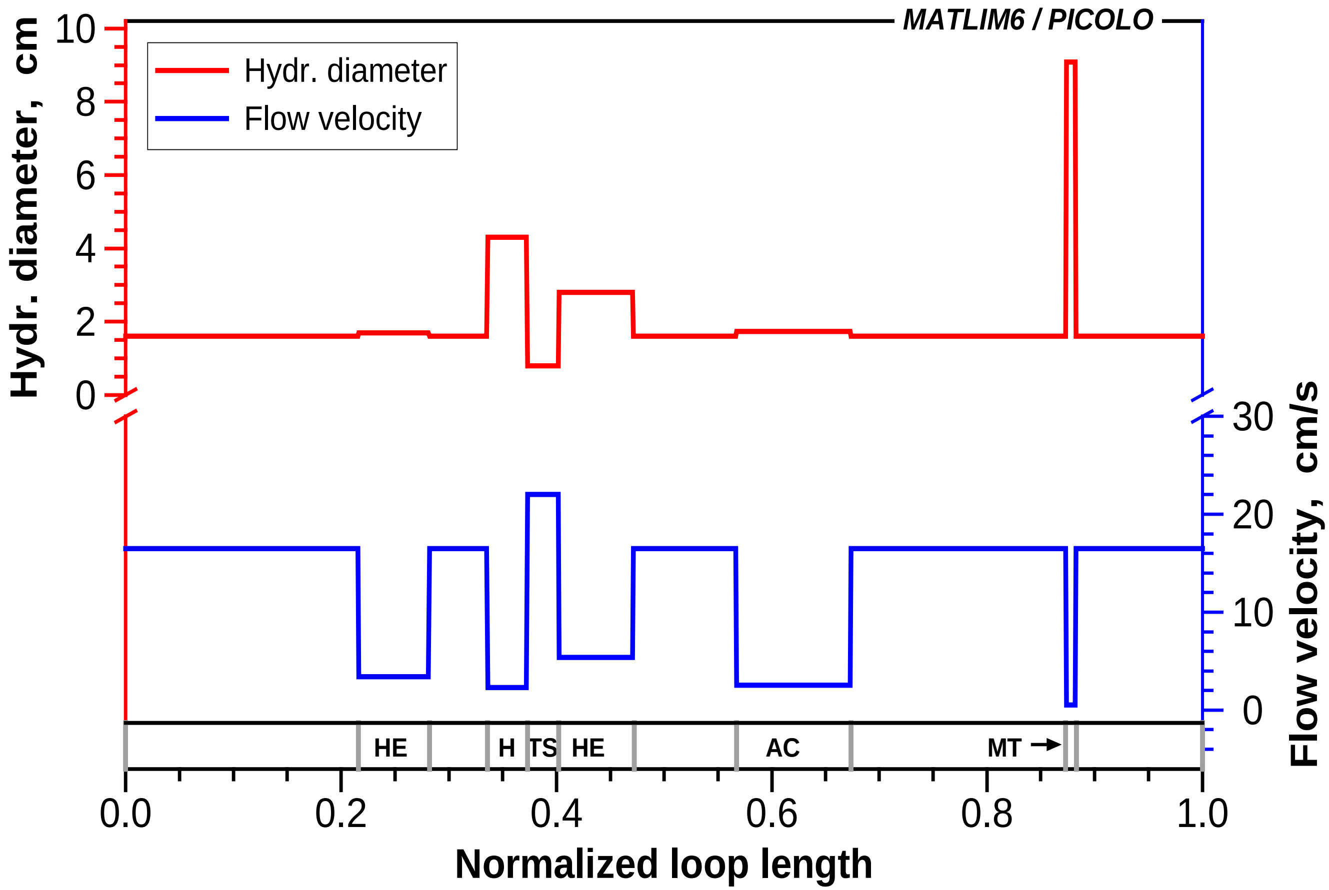


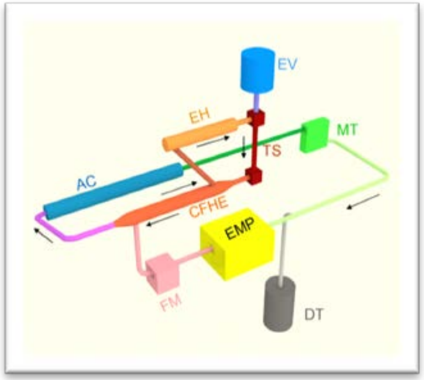

# Modeling of Corrosion with MATLIM code for 550°C

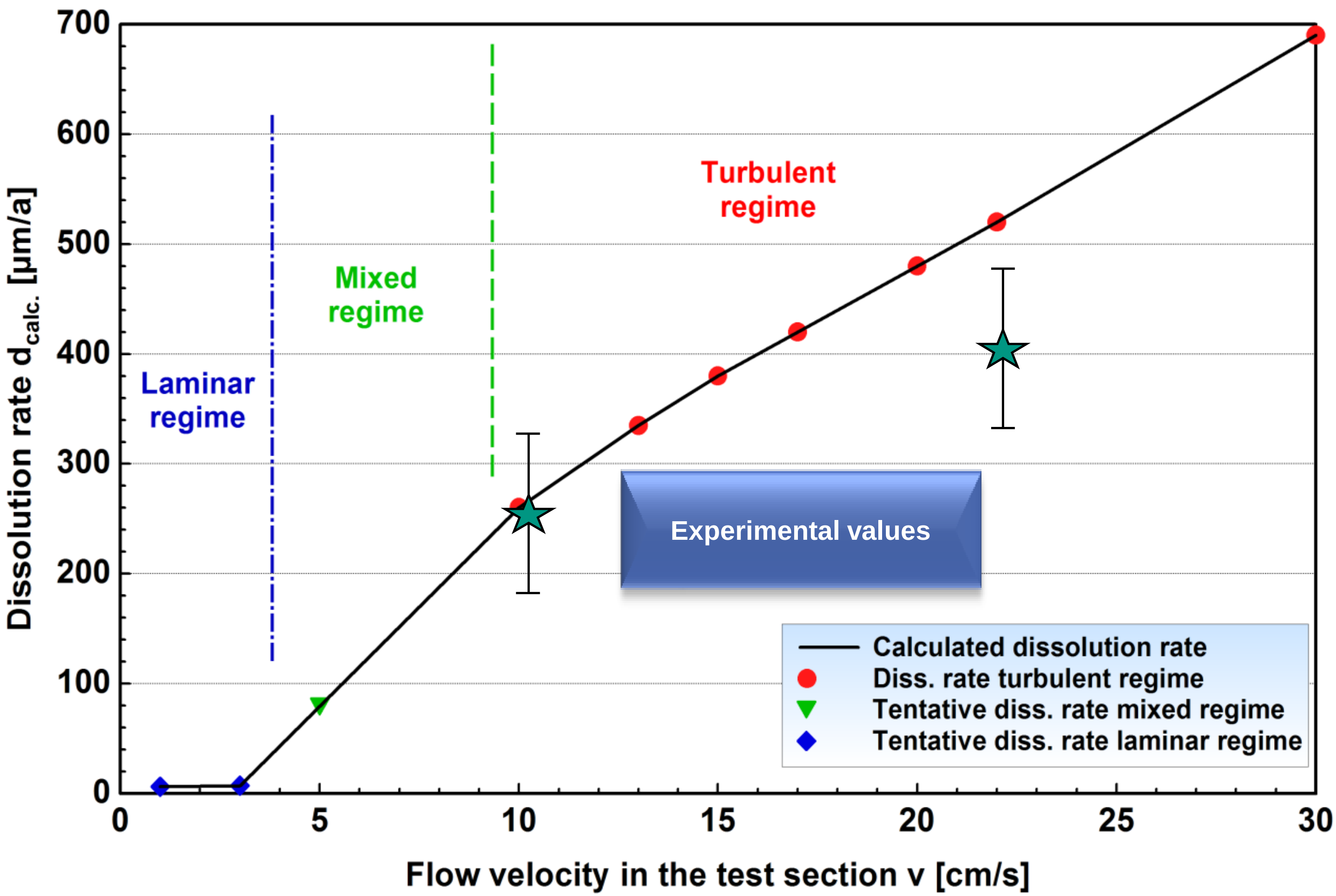

# Results of Corrosion Testing in PICOLO Loop EUROFER Steel Exposed to Pb-15.7Li;

## v = 0.1 m/s, 550°C

**Severe corrosion!!**

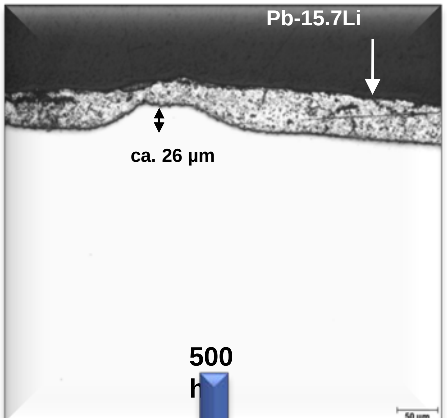


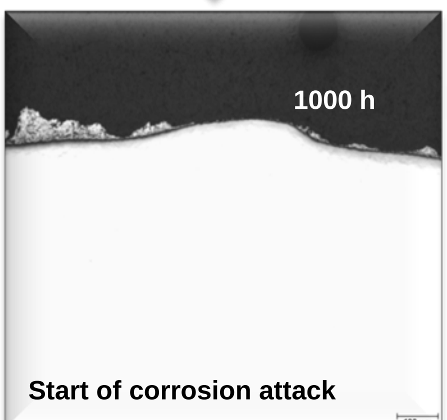


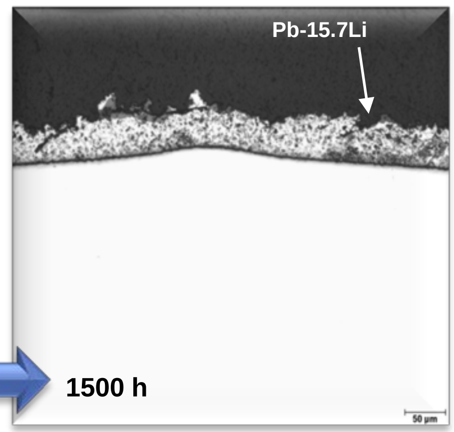


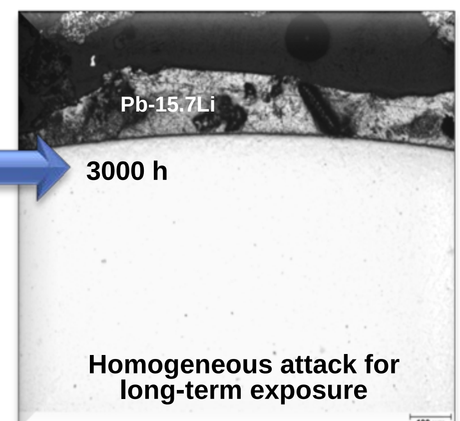

# Results of Corrosion Testing in PICOLO Loop at different flow rates

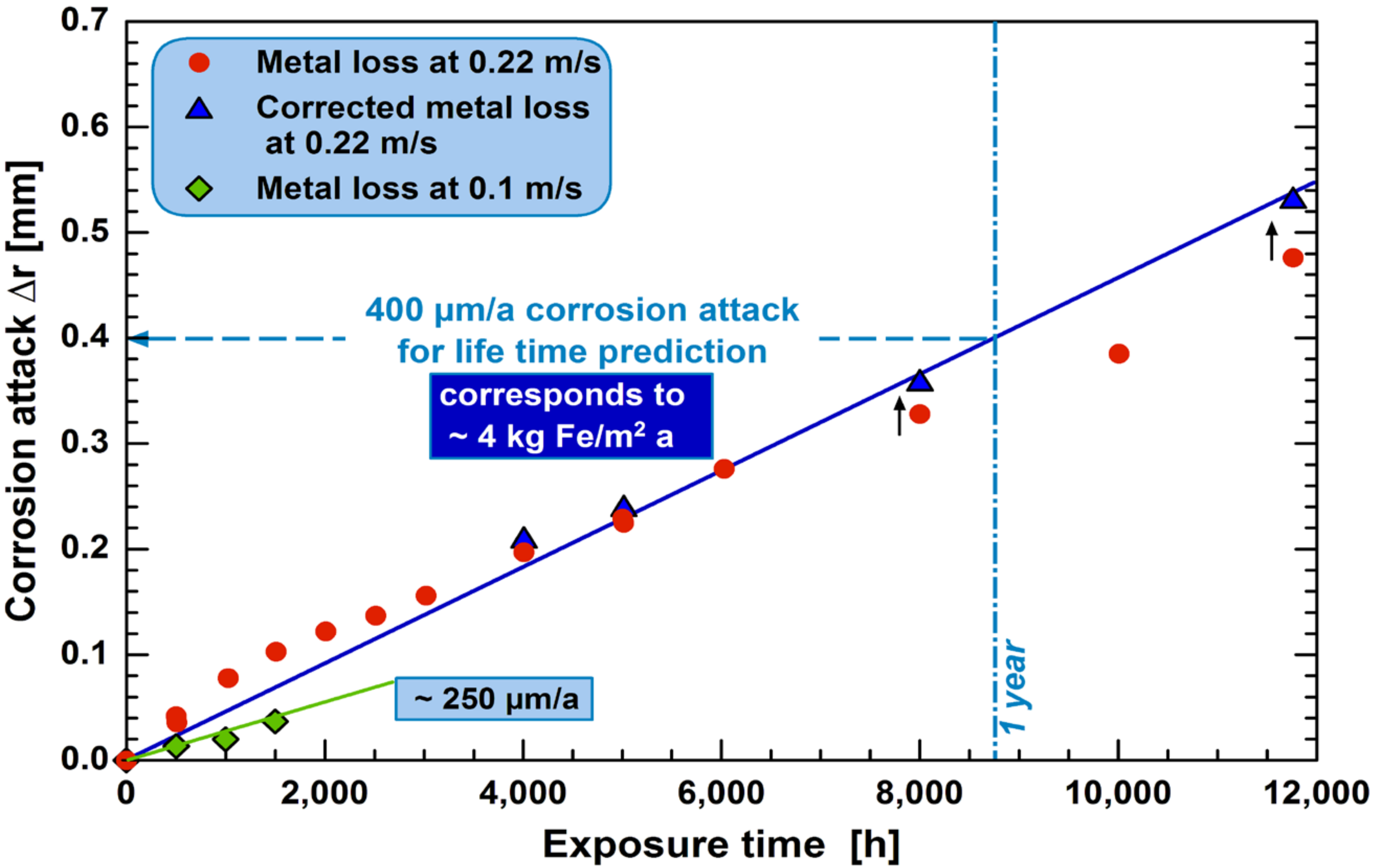

# Flow rate dependent corrosion of FM steels in Pb-15.7Li

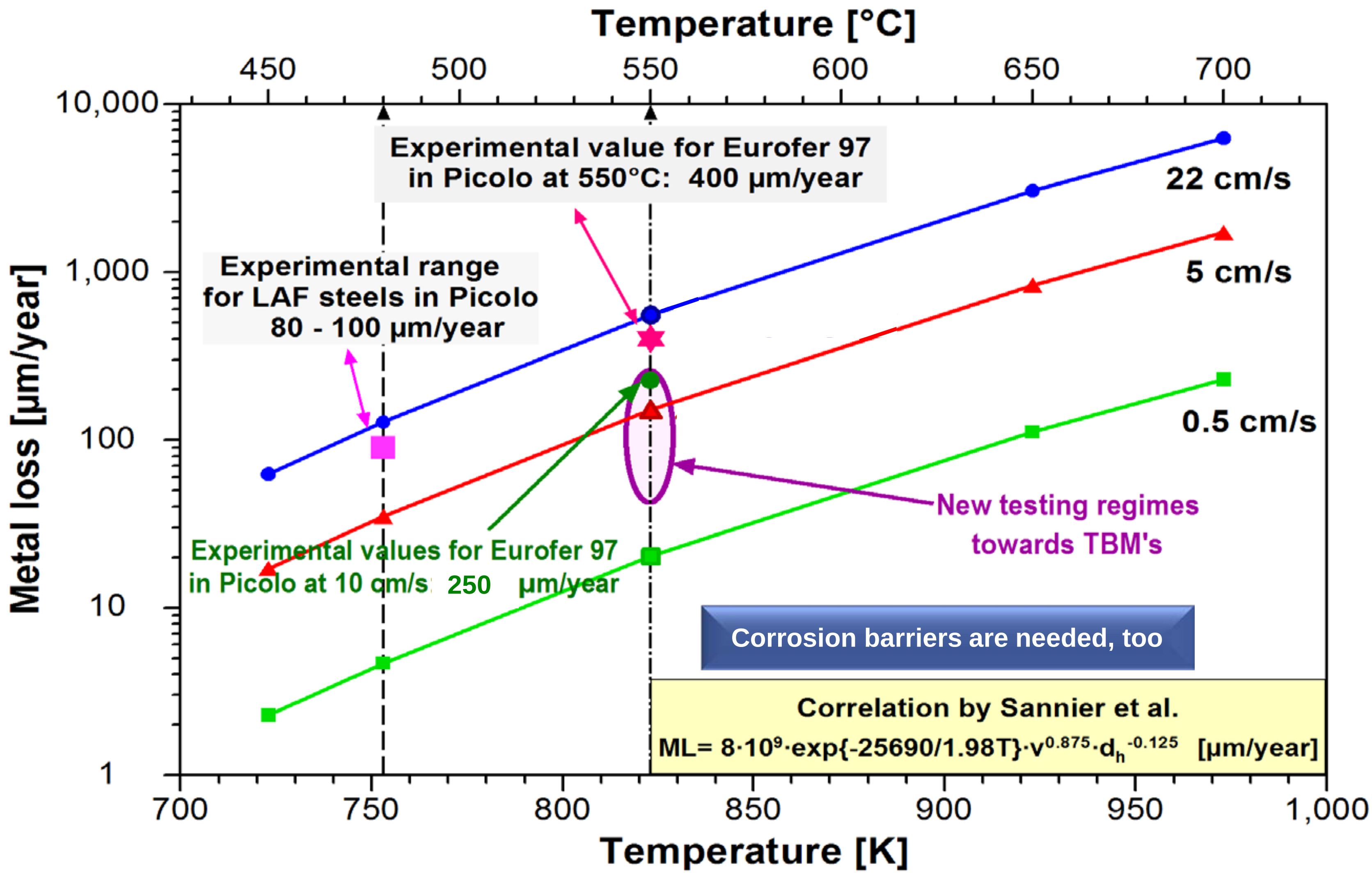

# Development of processes for Al-based anti-corrosion and T-permeation barriers for HLM environments

**Outline**

- T-permeation and/or anti-corrosion barriers for the HCLL-TBM in ITER (and for DEMO?)
  → why **Al-based** barriers?
- Overview of previous coating activities, e.g., the **HDA** process
  → study of iron-aluminide formation during heat treatment
- New electro-chemical Al coating processes
  - **ECA**, Al deposition from organic aprotic electrolyte
  - **ECX** (X = Al, W, Ta …), deposition from ionic liquid + metal salt

# Investigated barrier systems

| Type of coatings | Thickness | Agency \| Country | Year reported |
|---|---|---|---|
| $FeAl+Al_2O_3$ | 150-180 µm | KIT, Germany (HDA) & CEA, France (CVD) | Feb - Sep '04 |
| $FeAl+Al_2O_3$ | 100 µm | JRC, Ispra, Italy (VPS) | 1998 |
| $Er_2O_3$, $Al_2O_3$, $W+Al_2O_3$ | 1 µm<br>1 + 0.5 µm | IPP, Germany (PVD) | Aug 2007 |
| $(Cr_2O_3+SiO_2)+CrPO_4$ | 80-200 µm | JAERI, Japan (CDC) | Nov 2007 |
| W | 10-120 µm | KIT, Germany (EC) &<br>CRPP, Switzerland (EC, PVD, PS) | June 2007 |

# Hot-Dip aluminizing process

**Parameters for hot dipping are:**

**Temperature $T_{dip}$ = 700°C, dipping time of 30 s in Ar-5%$H_2$**

**Microstructure of hot dipped surface**

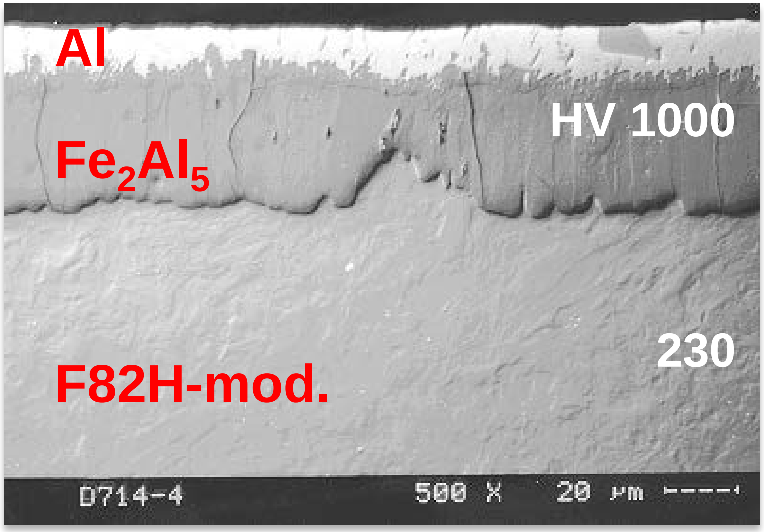


**The alloyed surface layer consists of brittle $Fe_2Al_5$,covered by solidified Al**

**Microstructure after heat treatment**

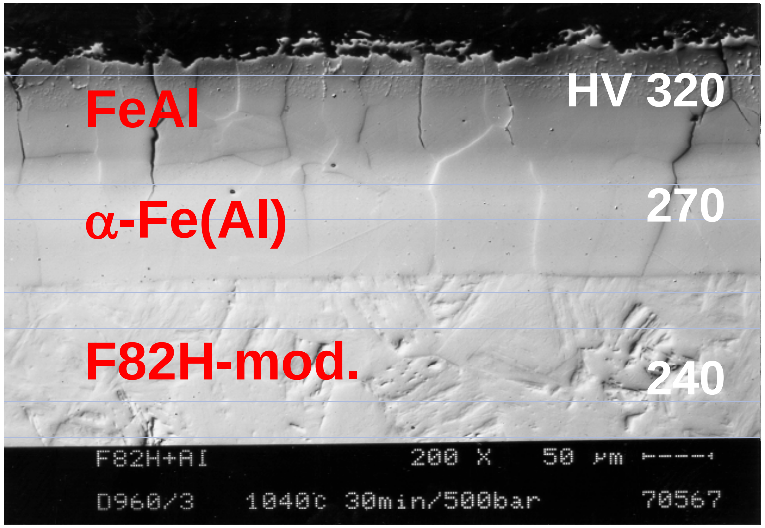


**Heat treatment at 980°C / 0.5 h + 760°C / 1.5 h and an applied pressure of >250 bar (HIPing) reduces porosity and transforms the brittle $Fe_2Al_5$-phase into the more ductile phases FeAl and α-Fe(Al)**

# Structure and technical requirements for an Al-based T-permeation barrier

**Requirements for a tritium permeation barrier**

- Reduction of T-permeation by a factor of <100 in Pb-15.7Li (1000 in gas phase)
- Self-healing of (mechanically) damaged layer must be thermodynamically possible in Pb-15.7Li (re-oxidizing)
- Long-term corrosion resistant in Pb-15.7Li up to ca. 550°C
- High content of low activation elements
- No negative influence on mechanical properties of the steel due to the coating process
- The coating process must be of industrial relevance

# Permeation data of HDA-coated FM-steels in $H_2$ and Pb-15.7Li (disk and tube samples)

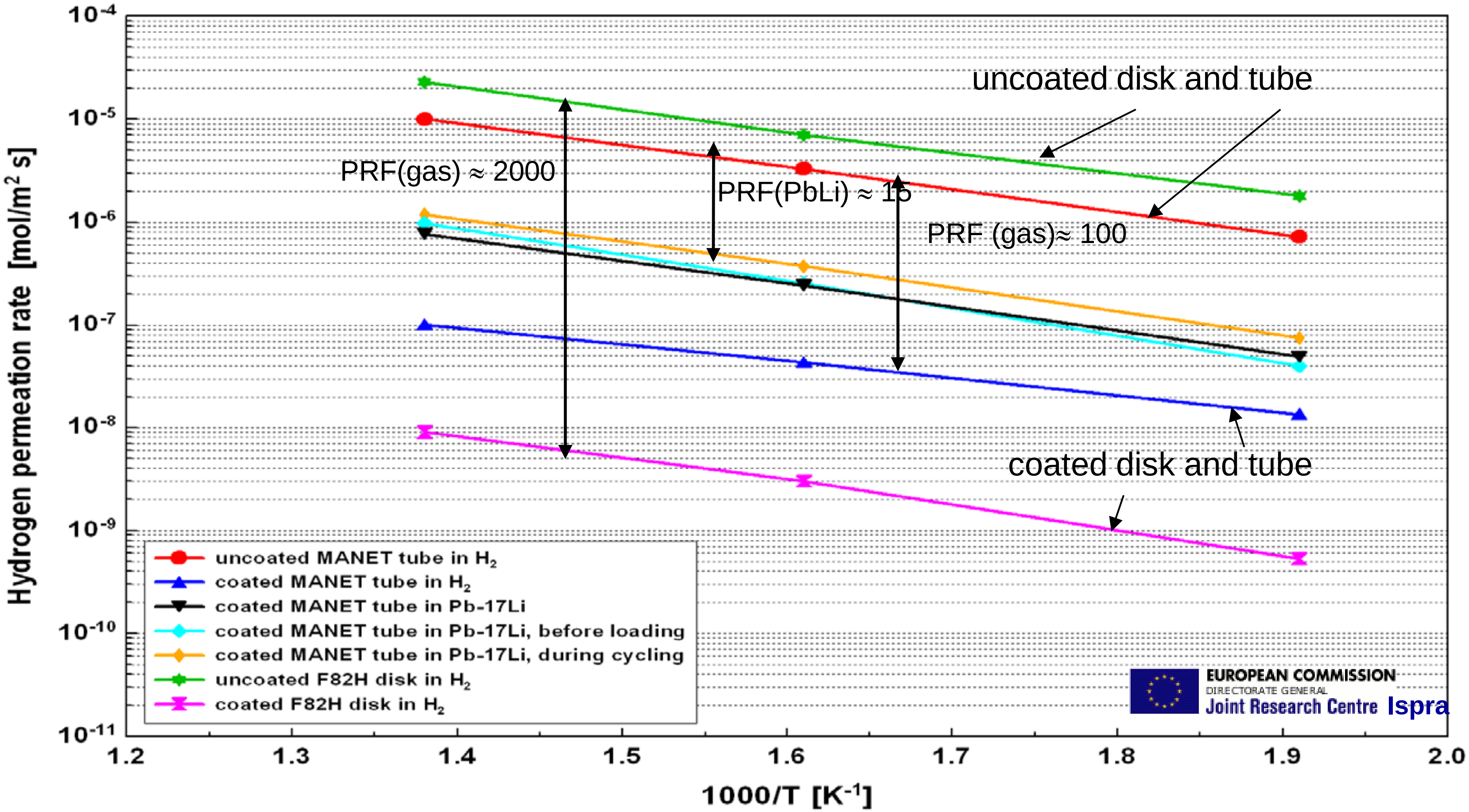

# Thermodynamics of $Al/Al_2O_3$-based T-permeation barriers

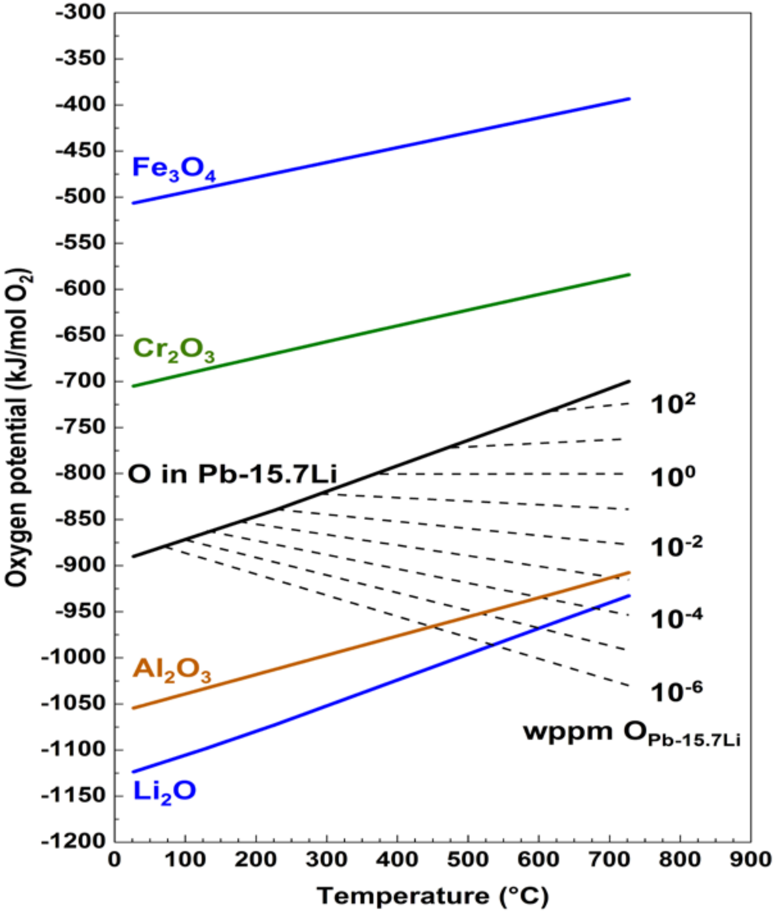


**Stability of oxides**

# Electro-chemical deposition for barriers/coatings
## - advantages of galvanic coatings -



### Why?

- **No gradients** $\Delta T$, $\Delta p$ (and resulting forces) between
  - electrolyte and metal surface
  - metal surface and bulk
  
  → no local heating as in EDM working
  
  → no mechanical load (no residual stresses)
- **High flexibility** in coating complex geometries

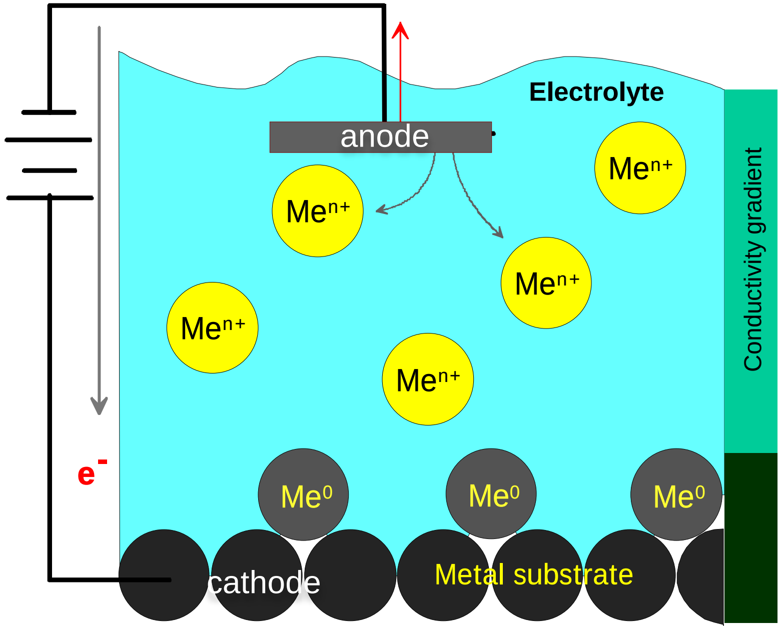


**Deposition scheme**

# Electro-chemistry for coating application

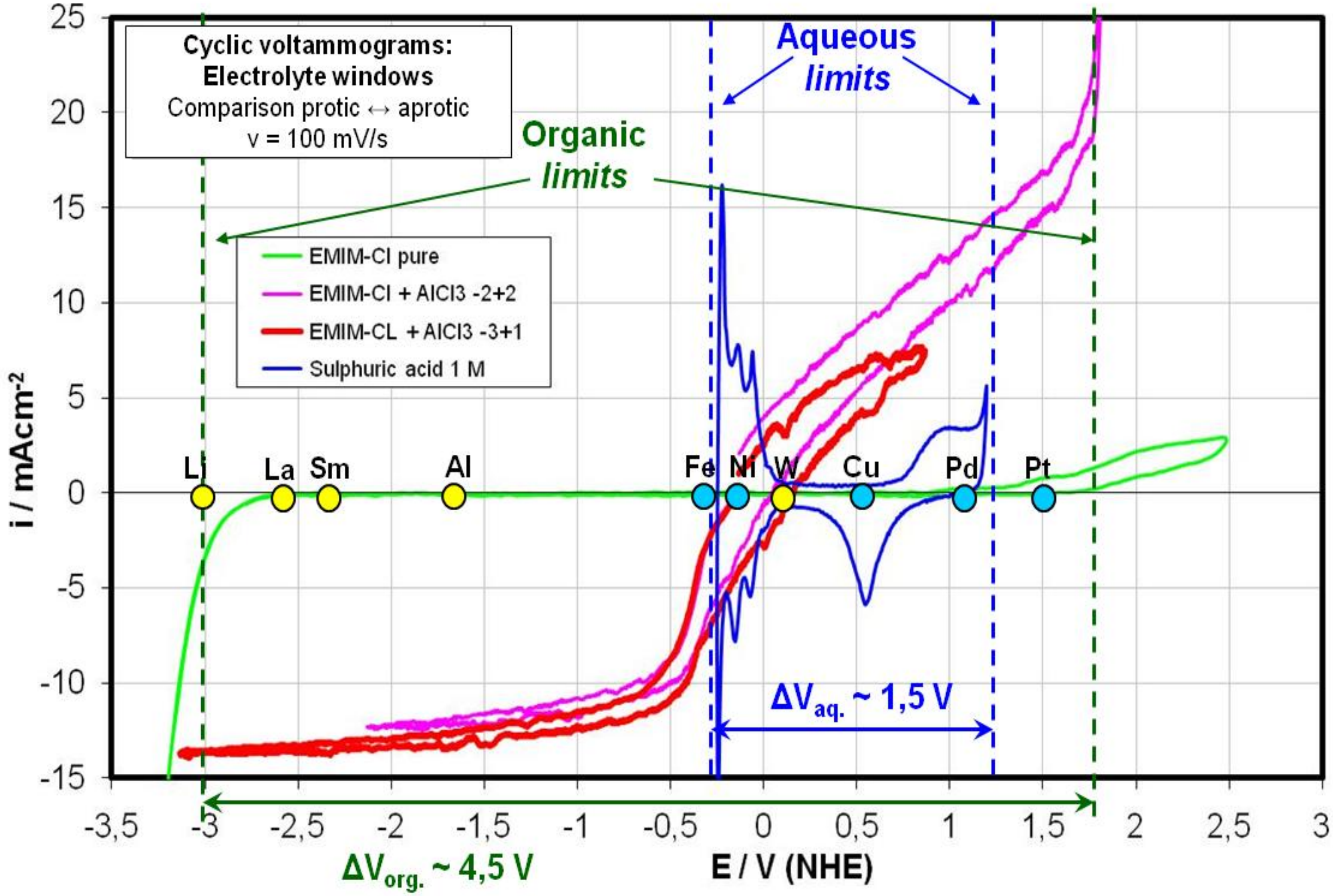


**EC measurements of protic and aprotic metal deposition systems**

# Electro-chemical aluminium deposition
## - properties of organic aprotic electrolyte systems -

| Solvens | | Toluol, Xylol<br>Diisopropylether | Quarternay Amin salts<br>e. g. Ethylmidazolium chloride |
|---|---|---|---|
| Ionic solubility of solvens | | **No** | **Yes** |
| Al-carrier system | | $KF \cdot 2Al(R)_3$<br>$R = C_nH_{2n+1}$ mit n= 2-6 | $AlCl_3$ |
| Temperature | | 100°C | RT … 200°C |
| Reactivity | Water | extremly high | modest |
| | Air | extremly high | low |
| | Temperature | modest | Stable up to 300°C |
| Toxicology \| biodegrability | | Aromates: ++/--- | Amines: -/+ |
| Max. conductivity [mS/cm] | | 19,5 | 22,0 |
| | | **ECA** | **ECX** |
| | | Al-Alkyl-Acryl-Complex in Toluol resp. Alkylether<br>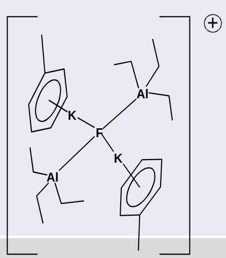 | $Al^{3+}$ + 3 Cl-<br>$\rightarrow$ EMIM-$AlCl_4$<br>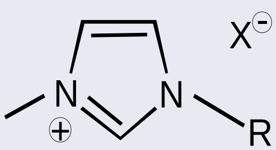<br> |

# Development of electro-chemical Al coating process (ECA)

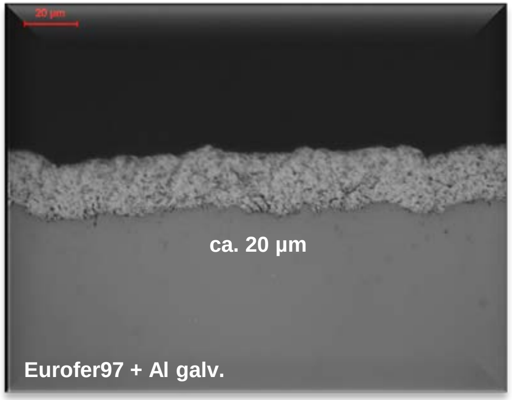


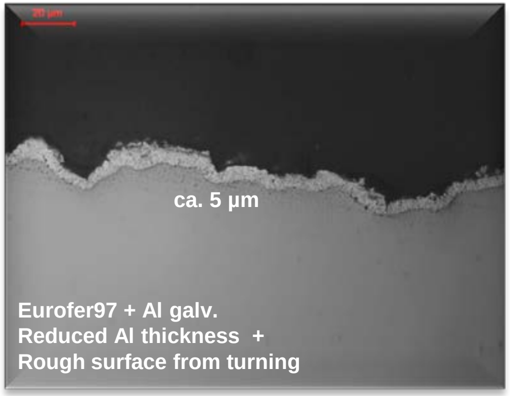


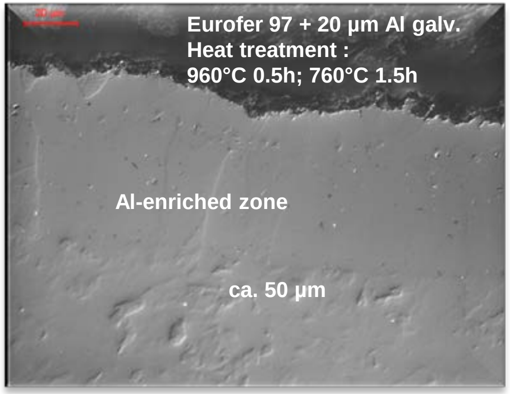


**Process specifics**

Organic electrolyte, Al-alkyle, under cover gas

Deposition temperature ca. 100°C, rate ≈ 12 µ/h

More complex geometries can be coated; even inside tubes

**Result of ECA development:**

- Electro-chemical coating applicable to functional scales in TBM's
- Barrier function tested in corrosion, successfully
- Salt-based processes have to be developed for higher compositional flexibility
- Reason: Electro-negativity of refractory metals and unique behavior

# SEM-EDX analyses of annealed Al-coated EUROFER by ECA

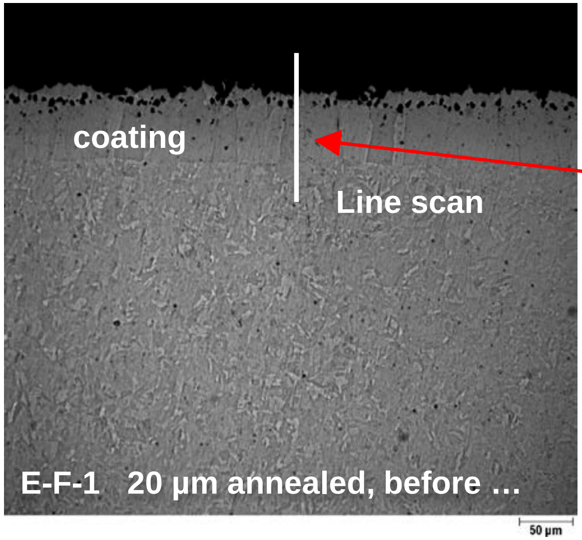


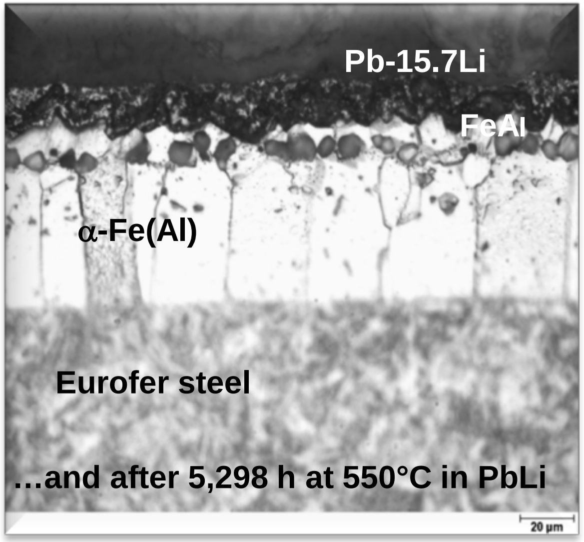


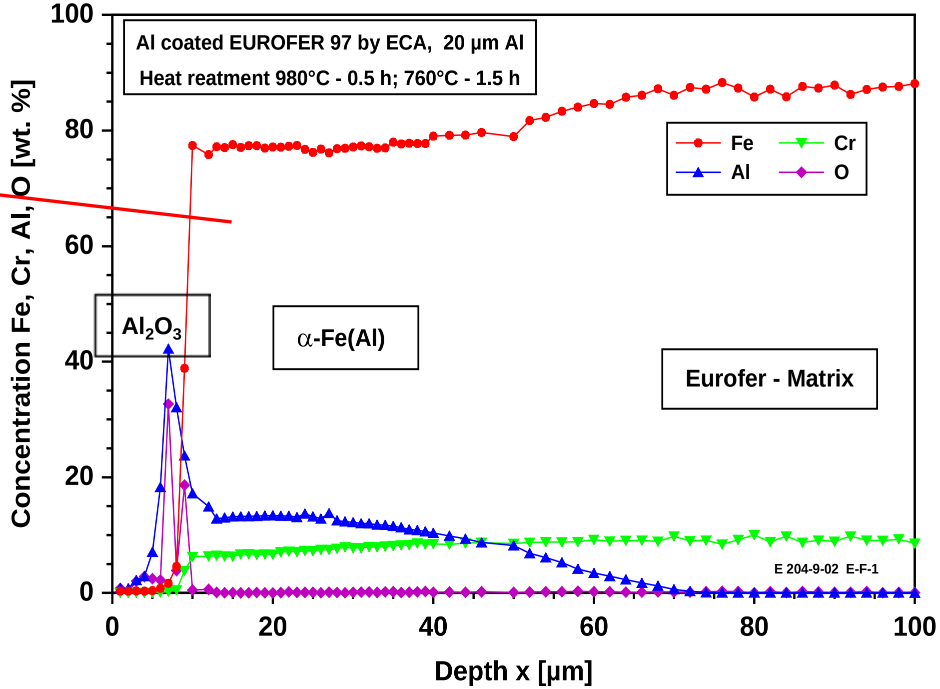

# Development of electro-chemical Al coating process (ECX, X=Al, W, Ta…)

**- Ionic liquids (IL's) + metal salts as new advanced electrolytes -**

**Ionic liquids as electrolytes**

- Structure like ionic salts (similar to solid ionic crystals: e. g. NaCl),100% ionic
- No additional solvent is necessary
- Mostly liquid at "room temperature" (≤ 100°C)

**Major properties**

- Thermally very stable (> 300°C) → low vapor pressure
- Not flammable
- High variability of chemical structure
- Good miscibility with inorganic metal salts as "carriers" for metal deposition, e.g. $AlCl_3$
- High electrical conductivity
- Electro-chemically very stable against oxidation and/or reduction
- High bio-compatibility

→ **IL's are superior for use for electro-chemical Al deposition**

# Electro-chemistry of aluminum in ionic liquids

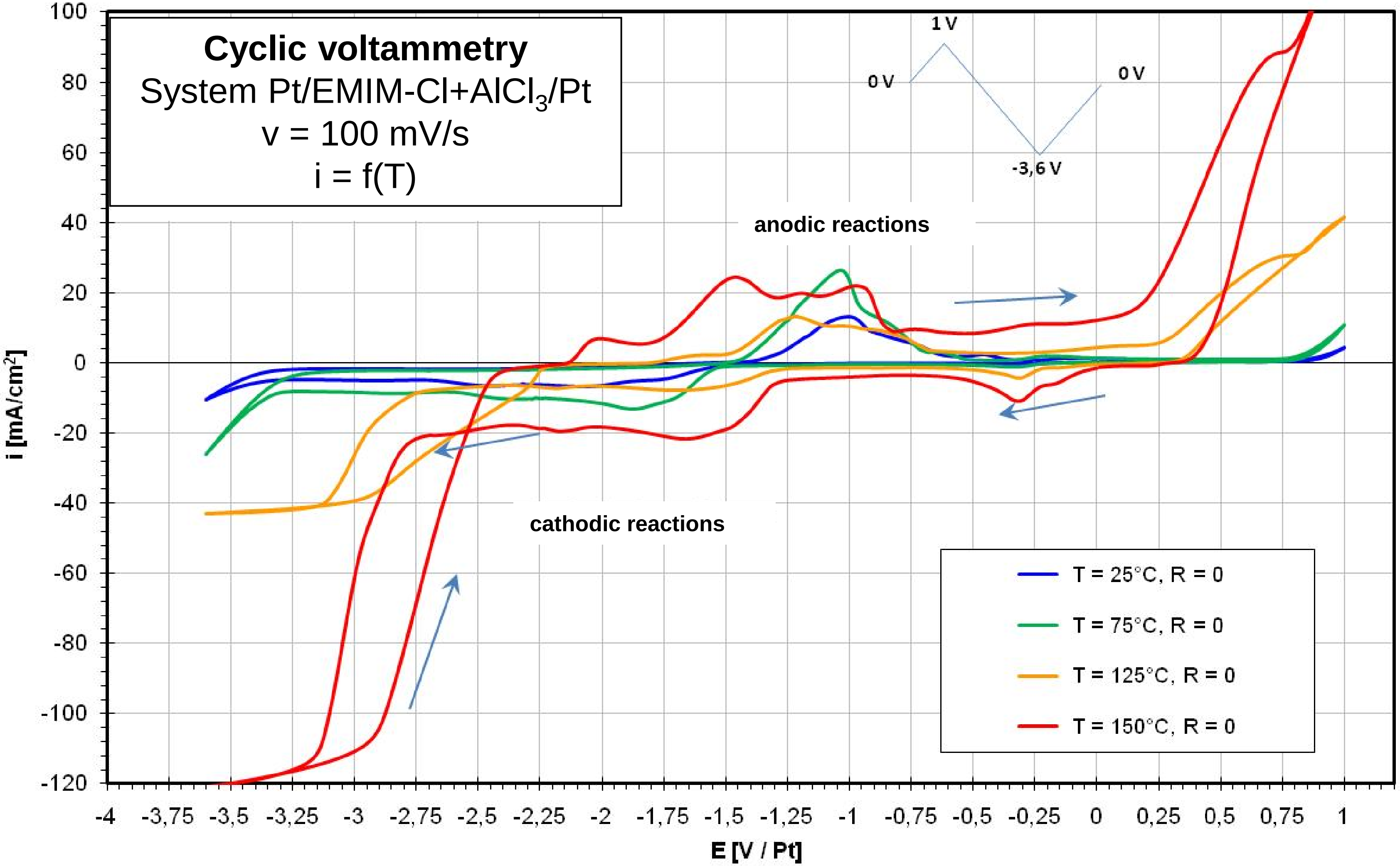

# Development of electro-chemical Al coating process (ECX)

**Process specifics for advanced electrolytes, e.g. ionic liquids**

| | |
|---|---|
| **Electrolyte:** | **EMIM-Cl + $AlCl_3$** |
| Atmosphere: | Ar cover gas |
| Deposition temperature: | ca. ≥ 100°C |
| Rate ≈ | 12 µ/h |

**More complex geometries can be coated e. g. inside of tubes**
**Industrial relevance for electro-deposition is given**

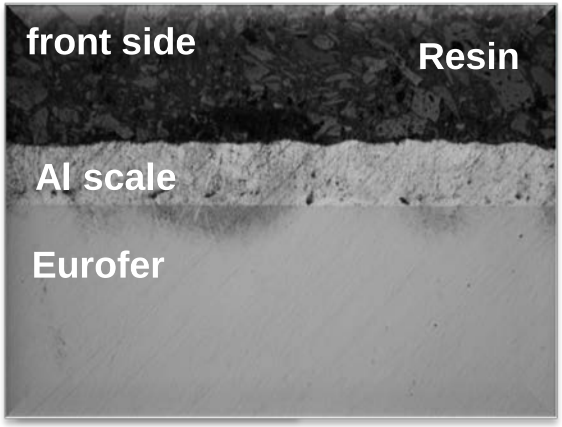


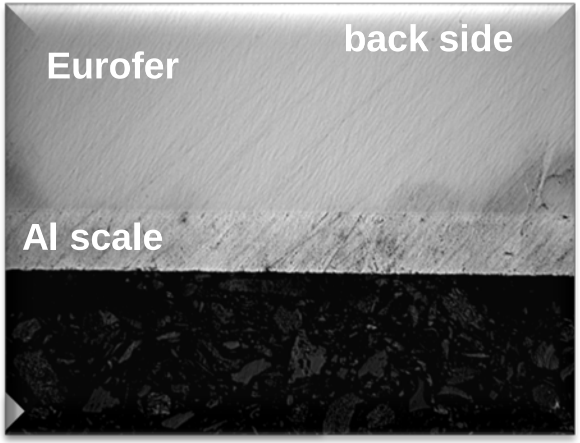


- **Process is reproducible**
- **Scale thickness controllable by current density and time**
- **Al scale on front and backside identical**

# Corrosion and Chemistry of Metallic Materials in Heavy Liquid (Lead) alloys

Karlsruhe Institute of Technology

**Typical corrosion mechanisms**

- Dissolution of alloying elements into the heavy liquid metal (W<<Fe, Cr<Ni)

  ⇒ **predominant corrosion mechanism in Pb-15.7Li**

- Mass transport of structural materials in the liquid lead alloys due to temperature gradients ⇒ dissolution in hot areas and precipitation in colder regions (heat exchanger, cooler, pumps etc.) ⇒ blocking of pipes

- Exchange of non-metals (O, N, C, H) between structural materials and liquid metals:

  ⇒ **in lead and LBE, it's mainly oxygen which affects the chemical stability by in-situ formed "protective" oxide scales**

- Erosion of structural materials in dynamic (fast flowing) systems

- Liquid metal embrittlement at low temperatures (with and without irradiation)

# Impact of oxygen dissolved in liquid lead and LBE on steel corrosion for Nuclear applications

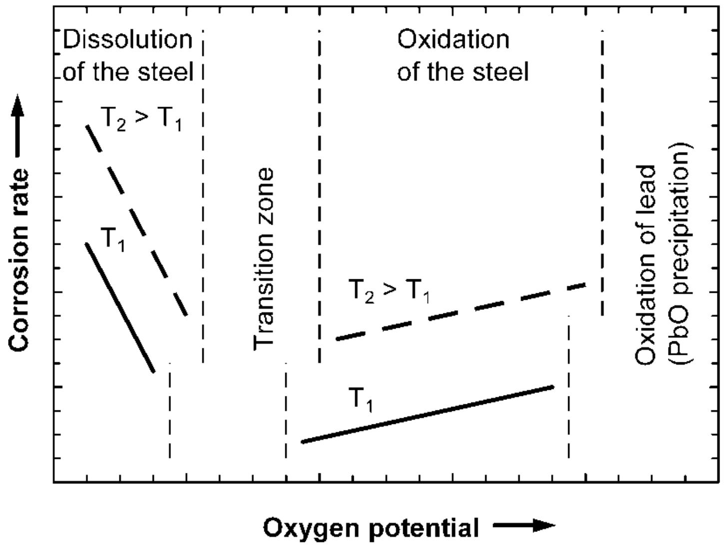


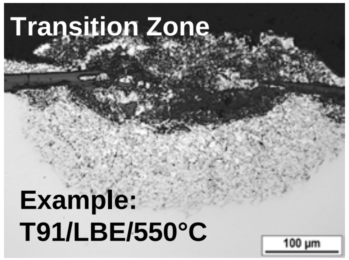


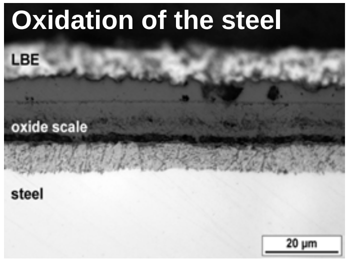


- Stimulation of the oxidation of steel constituents
  - Formation of an oxide scale on the steel surface
  - Separation of the steel from the liquid metal
  - Hence, reduced dissolution rate
- Steel elements must be less noble than the liquid metal
  - Applicable to Pb, lead-bismuth (LBE)
  - Not applicable to lead-lithium (Pb-15.7Li)
- Relevant to
  - Lead-cooled fast reactor (LFR)
  - Accelerator driven system (ADS)

# Components of an oxygen control system

## Sensors for on-line monitoring

Electrochemical oxygen monitoring

- Solid electrolyte on the basis of yttria-stabilized zirconia (YSZ)
- Metal/metal-oxide or Pt/gas reference electrode

Issues to be addressed (in general)

- Compatibility with the use in Pb alloys (YSZ/steel joint)
- Accuracy
- Long-term reliability

Licensing for nuclear application

- Structural stability of the YSZ product used
- Risk of contamination in case of electrolyte cracking

## Oxygen-transfer device(s)

“Classic“ mass transfer across the interface between oxygen source/sink and the liquid metal

| Type | Oxygen source | Oxygen sink |
|---|---|---|
| Solid-liquid | PbO | (less noble metals) |
| Gas-liquid | Ar, $H_2O$, air | Ar-$H_2$ |

**Long-term experience from operating experimental facilities for testing materials (steels) in oxygen-containing Pb alloys exists**

# Oxygen sensors developed at KIT

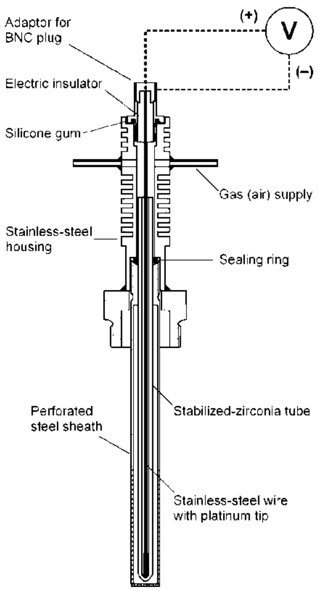


- Long electrolyte tube (Ø 6×255 mm)
- Polymer sealing ring in sufficient distance from the liquid metal
- Cooling fins for reducing the thermal load on the sealing ring
- Steel sheath for protecting the electrolyte from shear forces, serving as electric lead on the liquid-metal side
- Reference electrodes
  - (Steel)Pt/air
  - (Mo)Bi/$Bi_2O_3$

$U_{th}$ :
~3 mV at 300°C
~11 mV at 700°C (Mo/stainless steel)

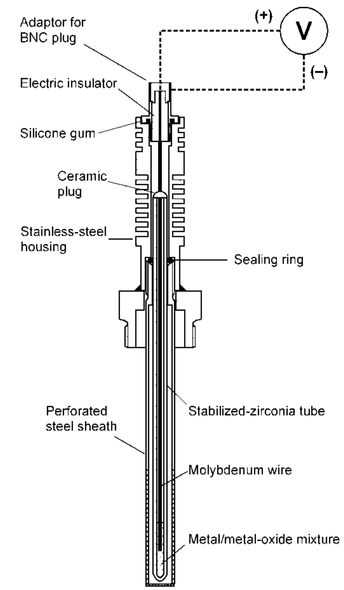


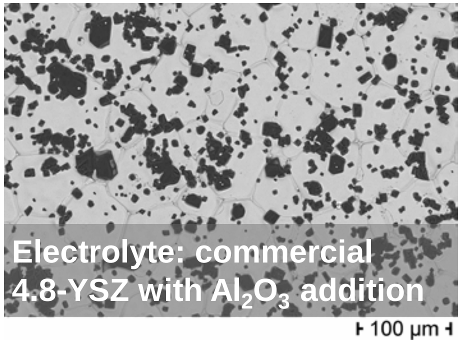


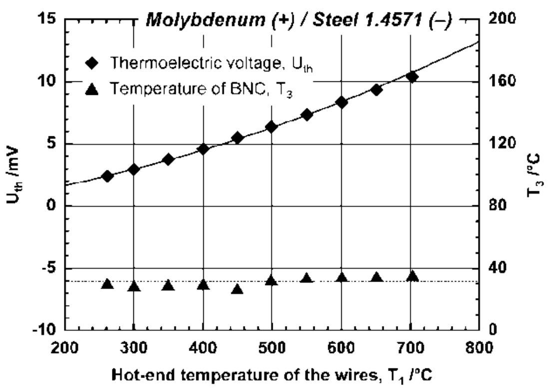

# Testing of the sensor accuracy

| Adjusting known oxygen potentials in LBE |
| --- |
| Pb/PbO (oxygen saturation) |
| Co/CoO |
| Fe/Fe-oxide equilibria |
| Fe and Co added in the form of powder |
| **Stabilization of these potentials using gases with varying oxygen partial pressure** |
| Ar |
| Ar + air |
| Ar + $H_2$ |
| **Temperature range: 350–700°C** |
| **Digital multimeter with high impedance >1GW** |
| **Sensors were tested without metallic sheath (Mo electrode as auxiliary electric lead), so as to minimize unintentional contamination of the LBE with metals.** |

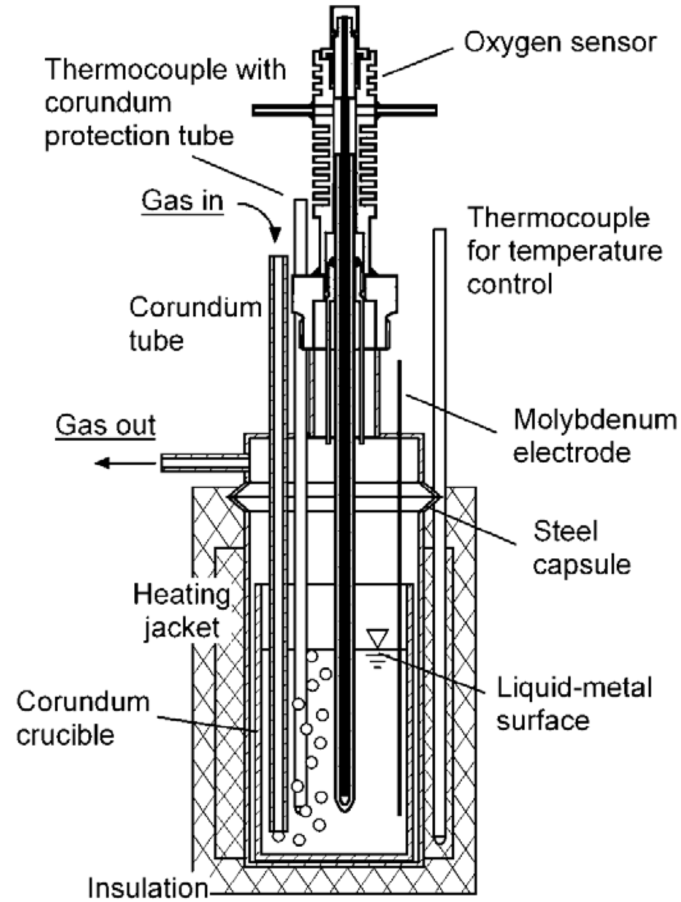

# Sensor accuracy required for efficient oxygen control

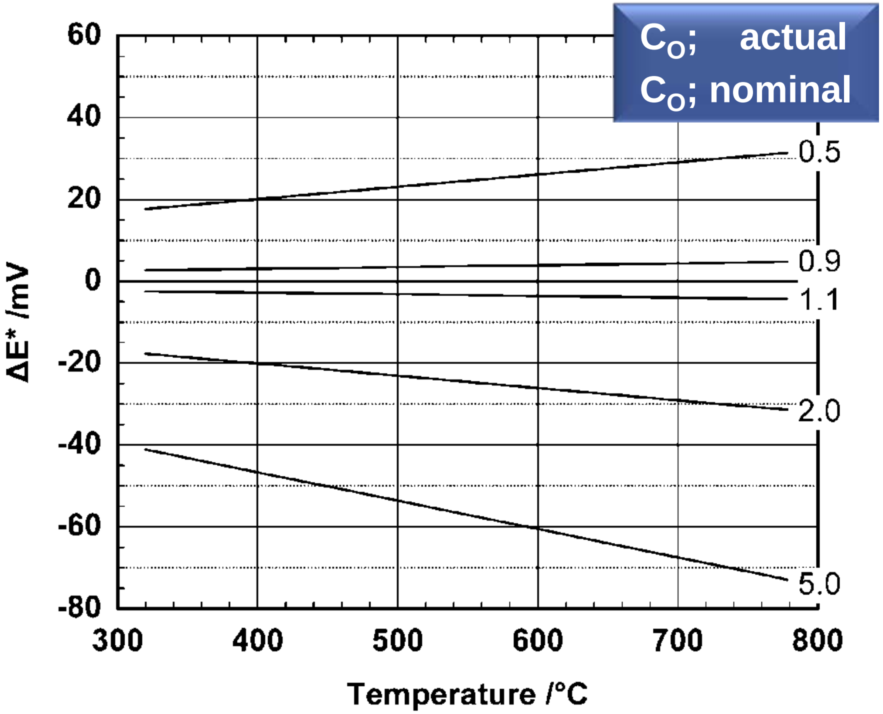


## Experience

- Half an order of magnitude in oxygen concentration can significantly change oxidation mechanisms for F/M steels
- Reproducibility under service conditions better than +20 mV/-45 mV at 400°C and +30 mV/ -65 mV at 700°C is needed

## Minimum requirement:

- Better than ± 20 mV at 400°C; ± 30 mV at 700°C
- Range of actual $c_O$ from 0.5 to 2 $c_{O;nominal}$

## Practical limit:

- ± 5 mV, corresponding to ± 10% in $c_O$, resulting from uncertainty in thermodynamic data used for calculating reference potentials

# Pt/air sensor and voltmeter with $R_V$ > 1GΩ

**Accuracy of measurement resulting from comparison with metal/metal-oxide equilibria adjusted in LBE**

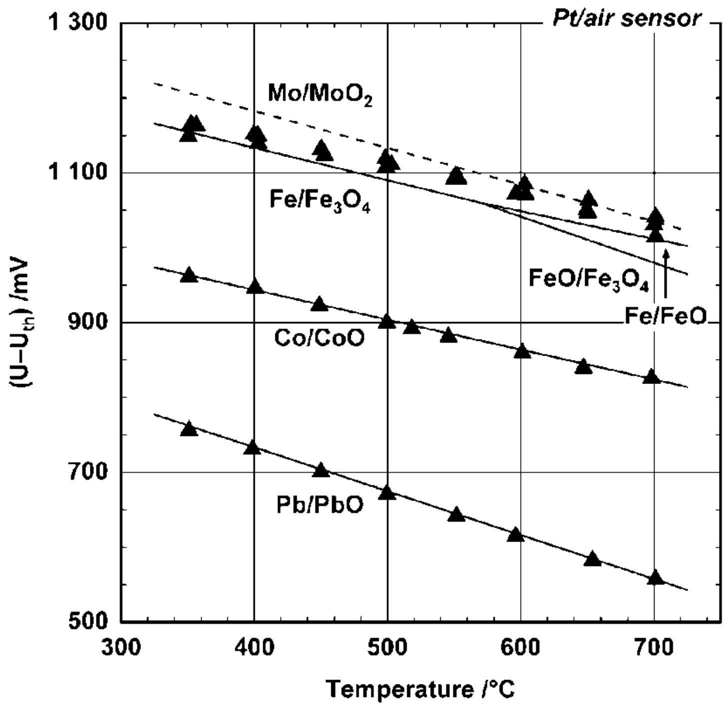


## Fe oxide equilibria

- Stepwise cooling or heating
- Ar-15% $H_2$ bubbling continuously through the LBE (5 ml/min) or quasi-stagnant
- Oxygen potentials move from Fe-oxide to Mo/$MoO_2$ equilibrium with temperature variation (Mo comes from wire submerged in the LBE)

## Co/CoO

- Stepwise cooling
- Ar 5.0 bubbling continuously through the LBE (5 ml/min)
- Periodically addition of air (5 ml/min) at 700 and 650°C
- Maximum deviation from theoretical prediction < 6 mV

## Pb/PbO

- Stepwise cooling
- Ar 5.0 bubbling continuously through the LBE (5 ml/min)
- Maximum deviation from theoretical prediction < 4 mV

# Bi/$Bi_2O_3$ sensor and voltmeter with $R_V$ > 1GΩ

**Accuracy of measurement resulting from comparison with metal/metal-oxide equilibria adjusted in LBE**

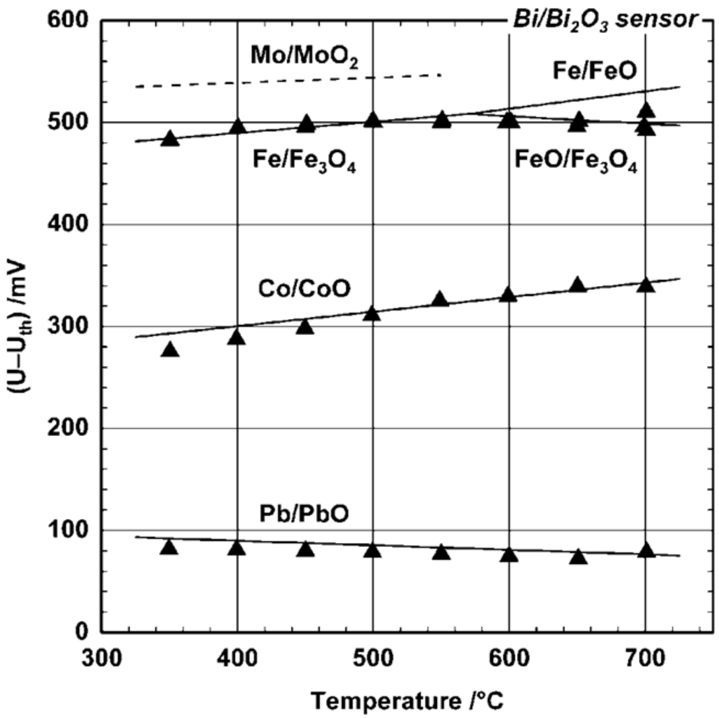


## Fe oxide equilibria

- Stepwise cooling or heating
- Ar-15% $H_2$ mostly quasi-stagnant
- Maximum deviation from theoretical prediction < 8 mV

## Co/CoO

- Stepwise cooling
- Ar 5.0 bubbling continuously through the LBE (5 ml/min)
- Maximum deviation from theoretical prediction < 15 mV

## Pb/PbO

- Stepwise cooling
- Ar 5.0 bubbling continuously through the LBE (5 ml/min)
- Maximum deviation from theoretical prediction < 8 mV

# Long-term performance of oxygen sensors in the LBE loop CORRIDA

- Criterion for proper operation ("plausibility")
  - Comparison of the output of all operating sensors on the basis of the calculated $c_O$
  - In consideration of possible oxygen consumption and expected accuracy of the sensors

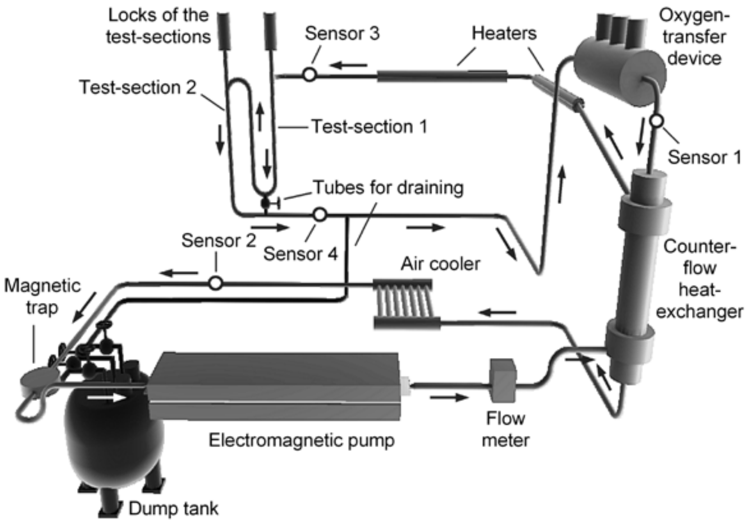


CORRIDA loop for materials testing in flowing oxygen-containing LBE

## Longest operating times

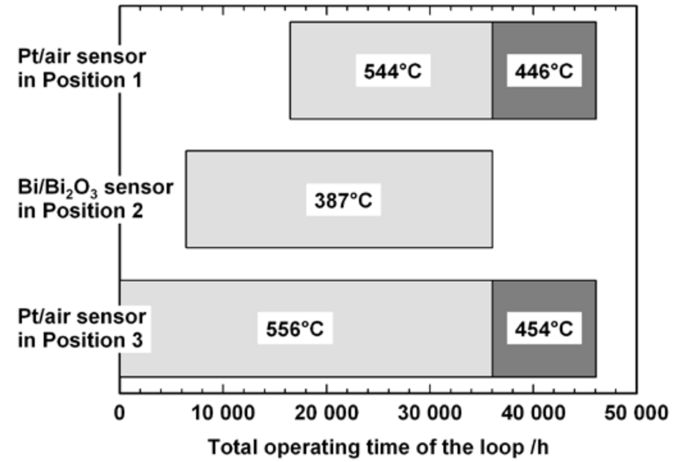


- Observed types of malfunction
  - Cracking of the electrolyte
  - Drifting of the sensor output to higher voltage, corresponding to lower $c_O$ (several orders of magnitude!)
    → Fouling of the electrolyte surface?
  - Pt/air sensors are less prone to cracking and did not show drifting of the output

# Oxygen transfer from gas to flowing LBE at 550°C

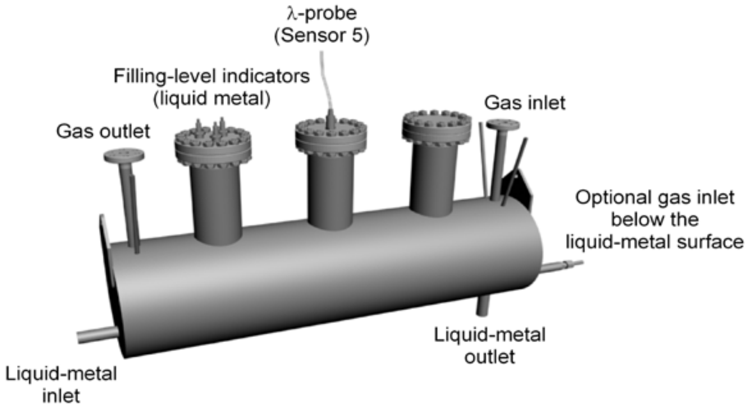


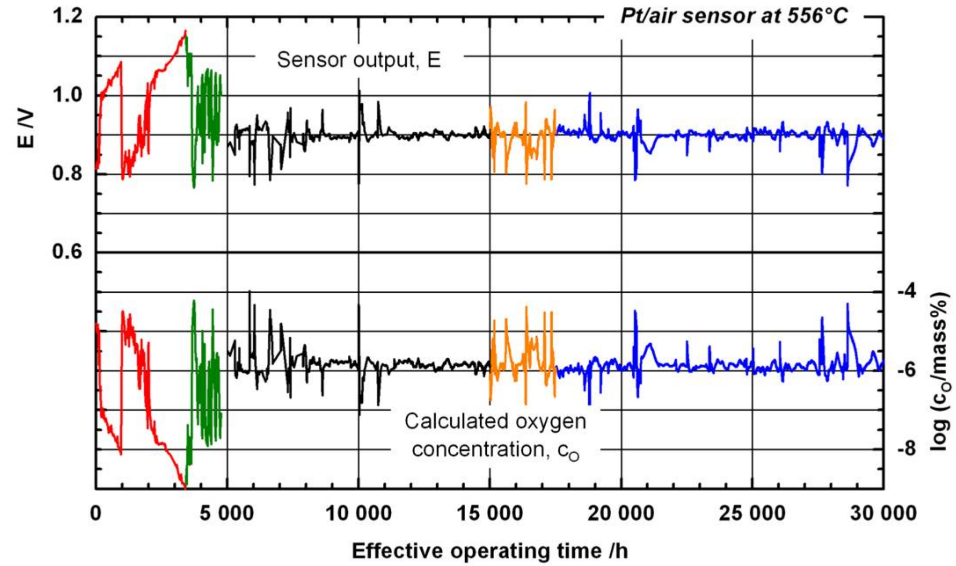


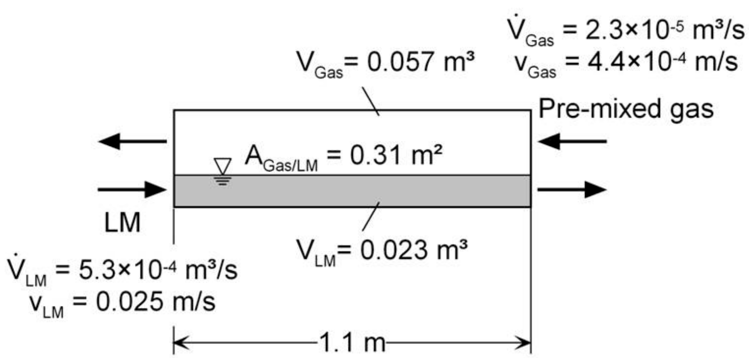


- Ar + Ar-5%$H_2$ (135:1) humidified at 4°C
- Gas flow: 500 cm³/min (referred to 25°C)

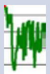

- Discontinous addition of air to humidified Ar-$H_2$

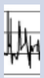

- Continous addition of 1-1.5 cm³/min air to humidified Ar-$H_2$

- 500 cm³/min dry Ar
- 1-1.5 ml/min air

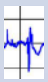

- 500 cm³/min Ar humidified at 18°C
- 1-1.5 cm³/min air

# Long-term corrosion studies in flowing oxygen-containing LBE conducted at KIT

| Temperature | Flow velocity | Nominal oxygen concentration | Maximum exposure times | Tested materials |
|---|---|---|---|---|
| 550 (+5)°C | 2 (±0.2) m/s | $10^{-6}$ mass% | ~ 20,000 h | CSEF (T91, E911, EUROFER), ODS steels, Type 316 SS, surface alloyed steels (Al), ... |
| 450 (+5)°C | 2 (±0.2) m/s | $10^{-6}$ mass% | ~ 8000 h | CSEF (T91, E911), pure Fe, Type 316SS, ... |
| Current exposure experiments: | | | | |
| 550°C | 2 m/s | $10^{-7}$ mass% | | |
| 450°C | 2 m/s | $10^{-7}$ mass% | | |
| 350°C | 2 m/s | $10^{-7}$ mass% | | |
| | | | | |
| Additionally, P92 and 15-15 CrNiTi (1.4970) | | | | |

# T91: Qualitative performance in oxygen-containing LBE at 550°C, v = 2 m/s and $c_O = 1.6\times10^{-6}$ mass% (I)

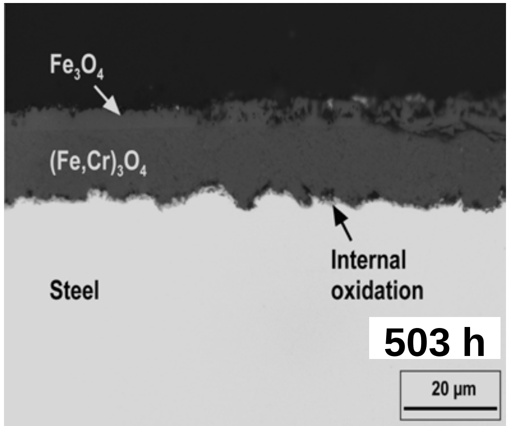


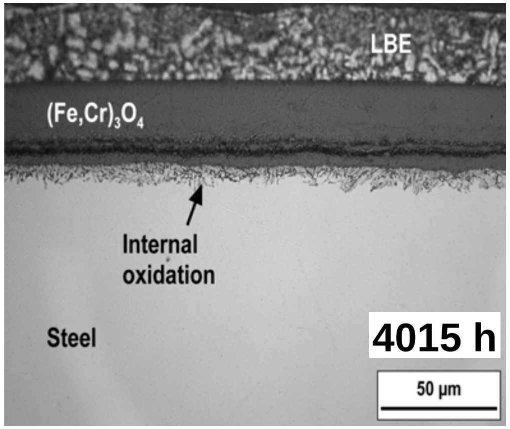


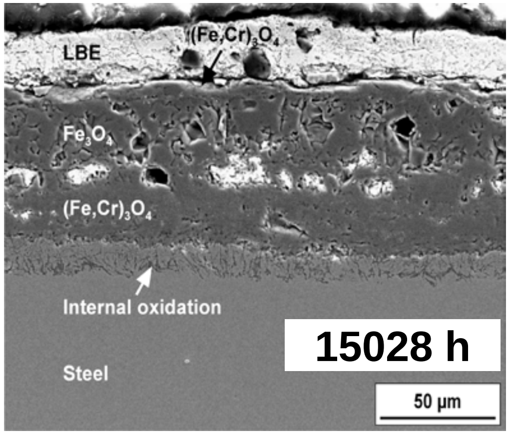


- Oxidation
- Oxide scale generally consists of
  - Magnetite ($Fe_3O_4$)
  - Cr-deficient spinel ($Fe(Fe_xCr_{1-x})_2O_4$)
  - Internal Oxidation Zone (IOZ)
- Magnetite is mostly missing, i. e., Fe is partially dissolved by the liquid metal (or eroded after $Fe_3O_4$ formation?)
- Inclusions of Pb and Bi inside the scale, especially after long exposure times

# T91: Quantification of oxidation in oxygen-containing LBE at 550°C, v = 2 m/s and $c_O = 1.6 \times 10^{-6}$ mass% (II)

Karlsruhe Institute of Technology

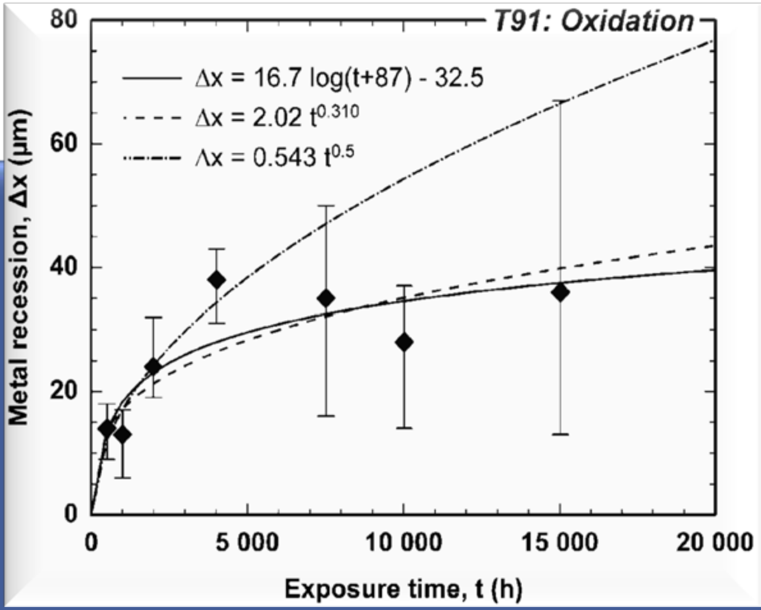


- Metal recession (loss of cross-section)
- Compromises the structural integrity of plant components
- Determined from measurements in the LOM (generally six measurements per investigated cross-section)
- Includes internal oxidation
- Local variation significantly increases with increasing exposure time
- Optimistic prediction: 50–70 µm after 100,000 h
- Worst-case: 100 µm after 4 years

# T91: Quantification of oxidation in oxygen-containing LBE at 550°C, v = 2 m/s and $c_O$ = 1.6×10$^{-6}$ mass% (III)

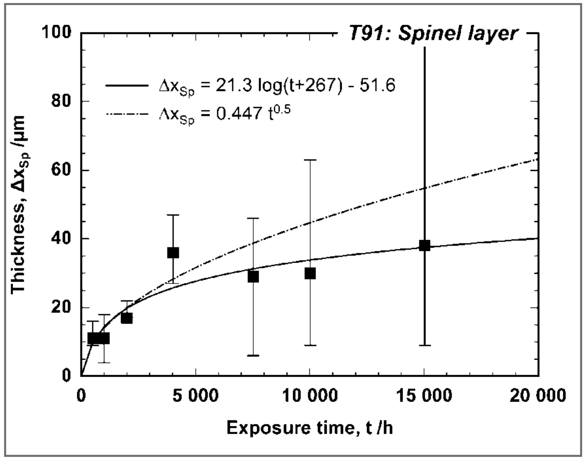


- Thickness of different layers of the oxide scale
- May affect heat transfer in the case of thermally-loaded plant components
- Generally twelve measurements per investigated cross-section
- Thickness of spinel layer significantly varies locally with increasing exposure time
- Average thickness of the spinel layer is in the order of the metal recession

Fe flux into the LBE can be estimated from the spinel layer thickness

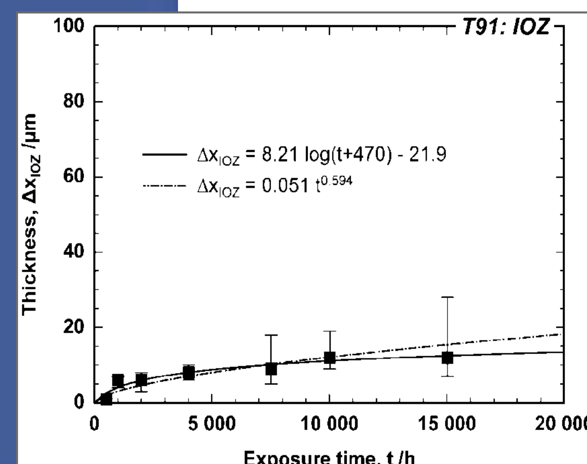

# Kinetics of oxide-scale growth for T91-B at 450°C, 2 m/s and $10^{-6}$ mass% oxygen (I)

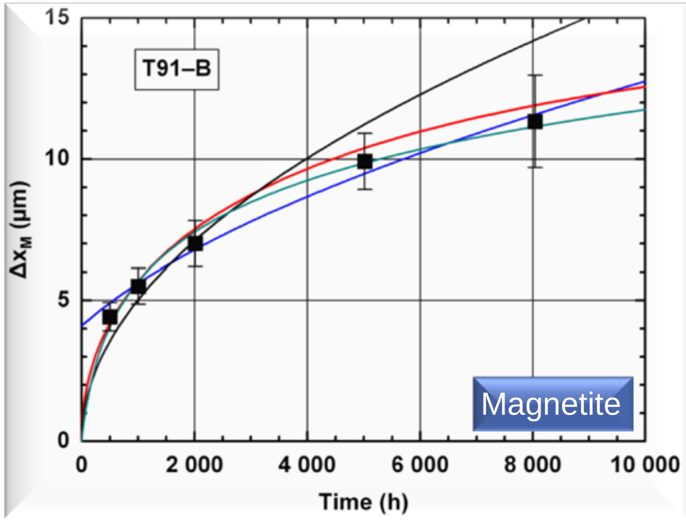


| | |
|---|---|
| **Parabolic:** | $\Delta x^2 = k_2 t$ |
| **Parabolic after faster initial kinetics:** | $\Delta x^2 = k_2 t + C_2$ |
| **Logarithmic:** | $\Delta x = k_{log} \log(t + t_0) + C_{log}$ |
| **Paralinear:** | $\frac{d\Delta x}{dt} = \frac{k_p}{d\Delta x} + k_1$ |

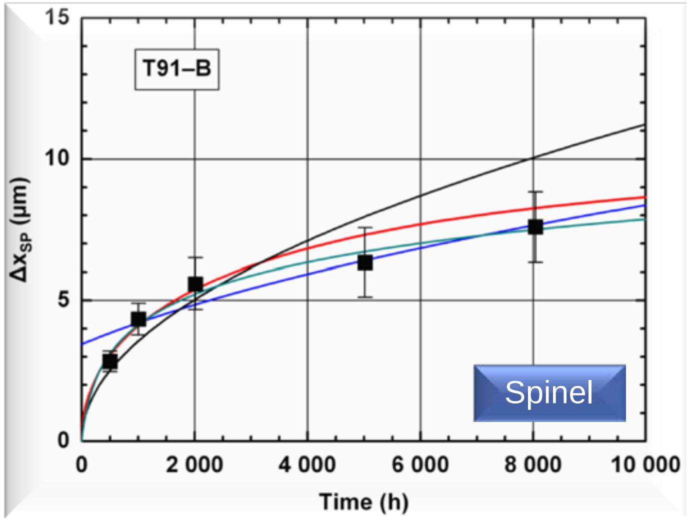


- **Local internal oxidation was not considered**
- **Thickness of the oxide layers slightly lower (by ~20%) for T91-A**

# Data extrapolation for T91 at 450°C, 2 m/s and $10^{-6}$ mass% oxygen (II)

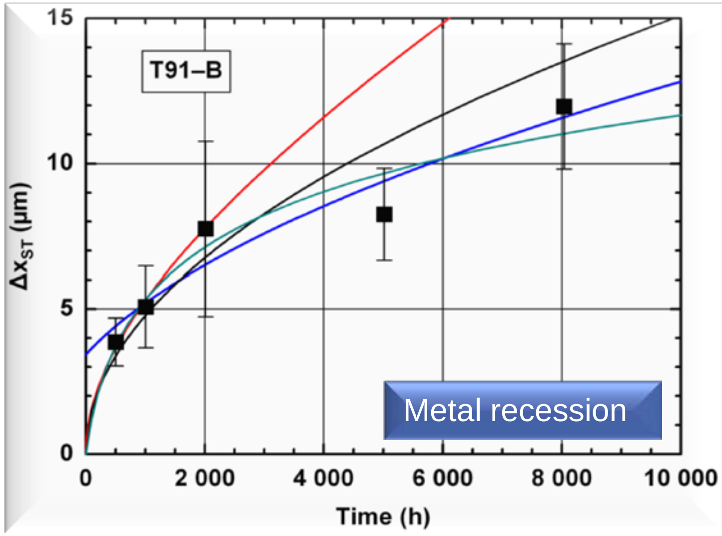


| | | |
|---|---|---|
| **Parabolic:** | **$\Delta x^2 = k_2 t$** | |
| **Parabolic after faster kinetics:** | **$\Delta x^2 = k_2 t + C_2$** | |
| **Paralinear model of oxide scale growth** | | |
| **Logarithmic:** | **$\Delta x = k_{log}(t + t_0) + C_{log}$** | |

| Exposure time (years) | 1 | 5 | 10 |
|---|---|---|---|
| **T91-A → Upper limit of Cr content specified for T9** | | | |
| $\Delta x_M$ (µm) | 10 | 13 – 22 | 13 – 31 |
| $\Delta x_{SP}$ (µm) | 7 | 8 – 14 | 8 – 20 |
| $\Delta x_{ST}$ (µm) | 9 | 20 | 28 |
| **T91-B → Lower limit of Cr content specified for T91** | | | |
| $\Delta x_M$ (µm) | 12 | 15 – 26 | 15 – 36 |
| $\Delta x_{SP}$ (µm) | 8 | 10 – 16 | 10 – 23 |
| $\Delta x_{ST}$ (µm) | 12 | 26 | 37 |

# Corrosion of martensitic ODS steel in LBE at 550°C (I)

## Influence of varying oxygen concentration

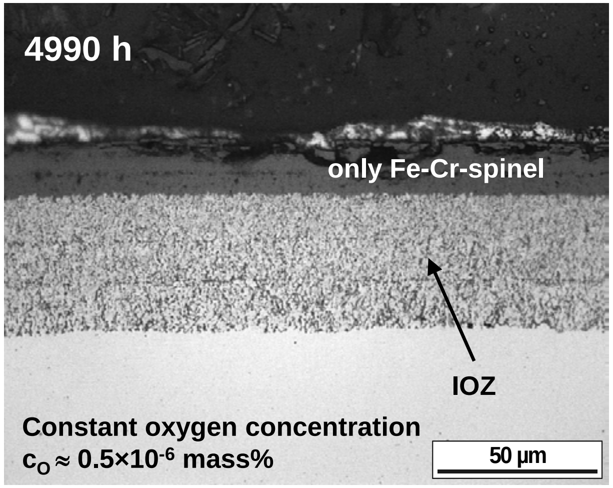


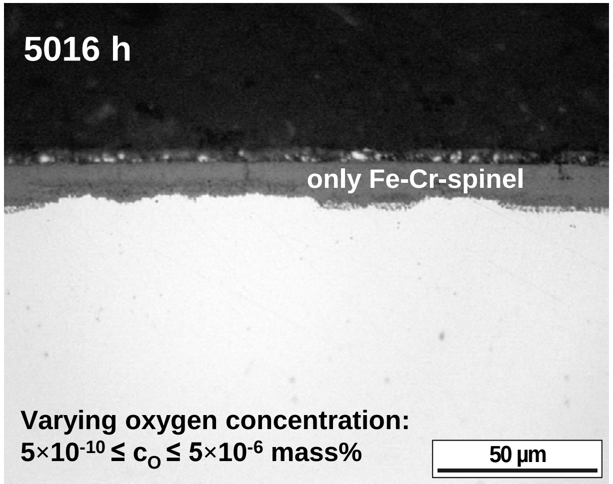


- Comparatively thin spinel scale (12µm)
- Significantly less internal oxidation
- Cr-enrichment in oxide at metal/scale interface

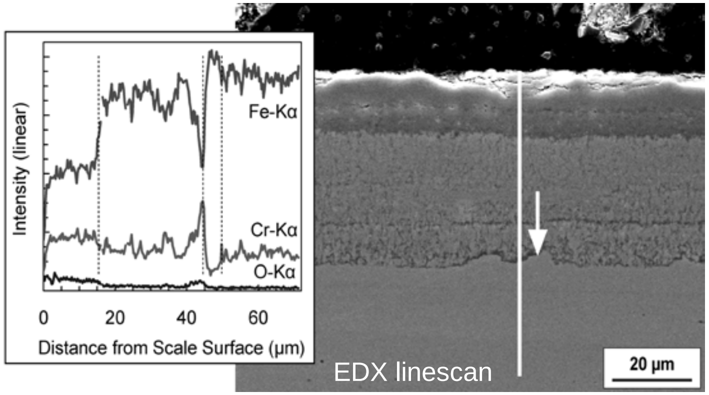

# Corrosion of martensitic ODS steel in LBE at 550°C

## Time dependence of oxidation under varying oxygen concentrations

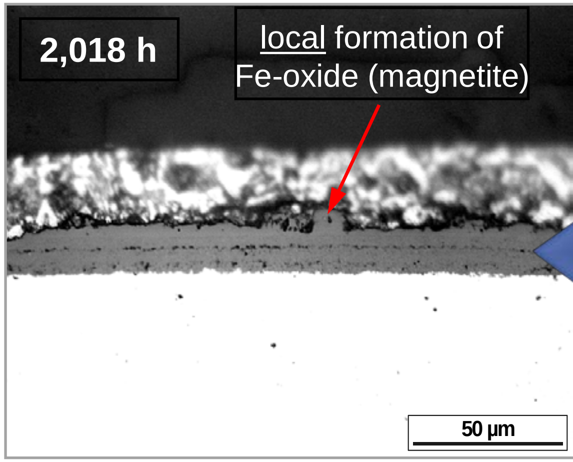


Cr-enrichment in oxide scale at metal/scale interface

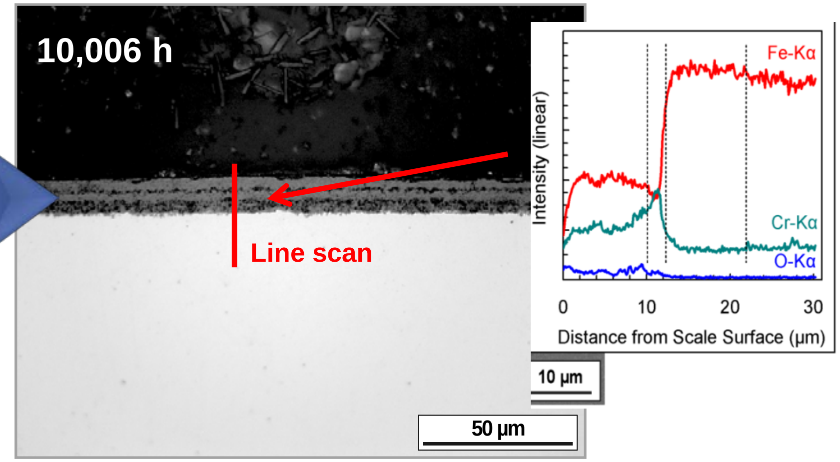


**Oxygen:**
$5\times10^{-9} \leq c_O \leq 5\times10^{-6}$ mass%

- Spinel scale (11 µm); local formation of Fe-oxide
- Little internal oxidation in comparison to scale formed at $c_O \approx 0.5\times10^{-6}$ mass%

**Oxygen:**
$5\times10^{-10} \leq c_O \leq 5\times10^{-6}$ mass%;
$c_O \approx 0.5\times10^{-6}$ mass% during the last 4990 h

- Comparatively thin spinel scale (11 µm) and little internal oxidation

Varying (mostly "low-oxygen") conditions during the first half of the exposure dominates the oxidation behavior

# Setting up of the new creep-rupture facility CRISLA for stagnant lead containing environment

## Creep-Rupture Facility for Tests in Na, Pb-17Li (basic construction)

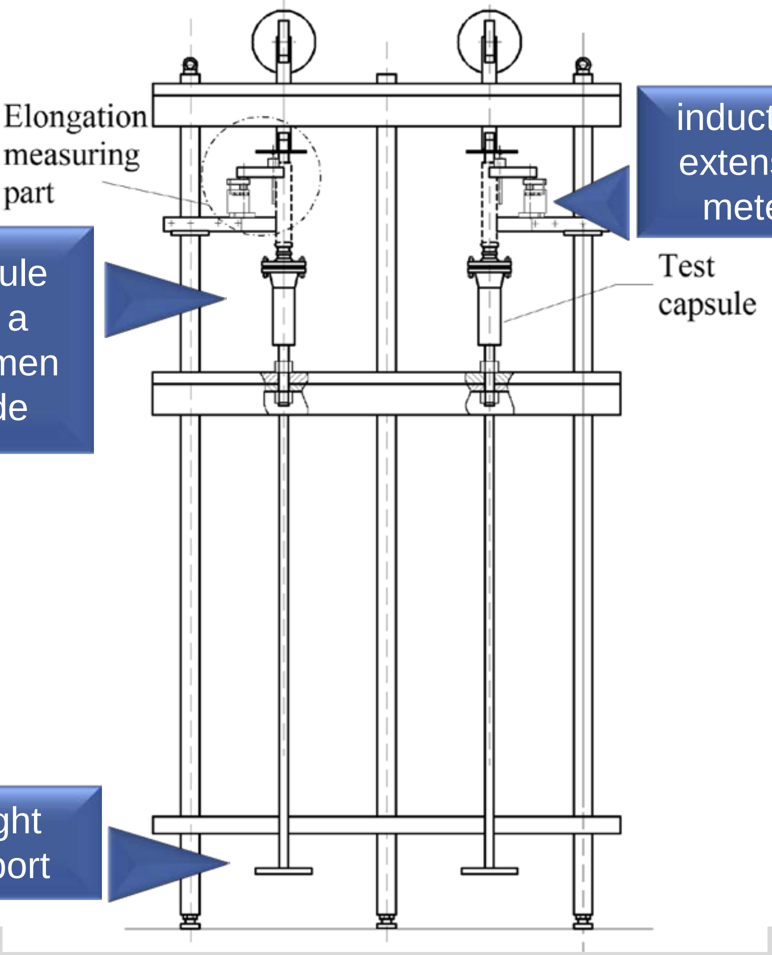


Capsule with a specimen inside

inductive extenso-meter

Weight support

# Setting up of the new creep-rupture facility CRISLA for stagnant lead containing environment

Karlsruhe Institute of Technology

## New designed creep-rupture capsule for CRISLA tests in Pb/LBE

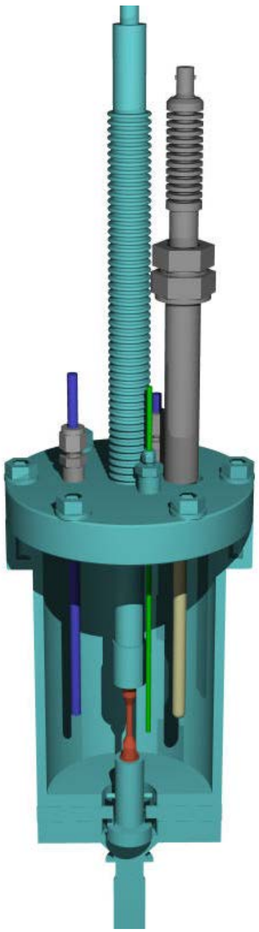

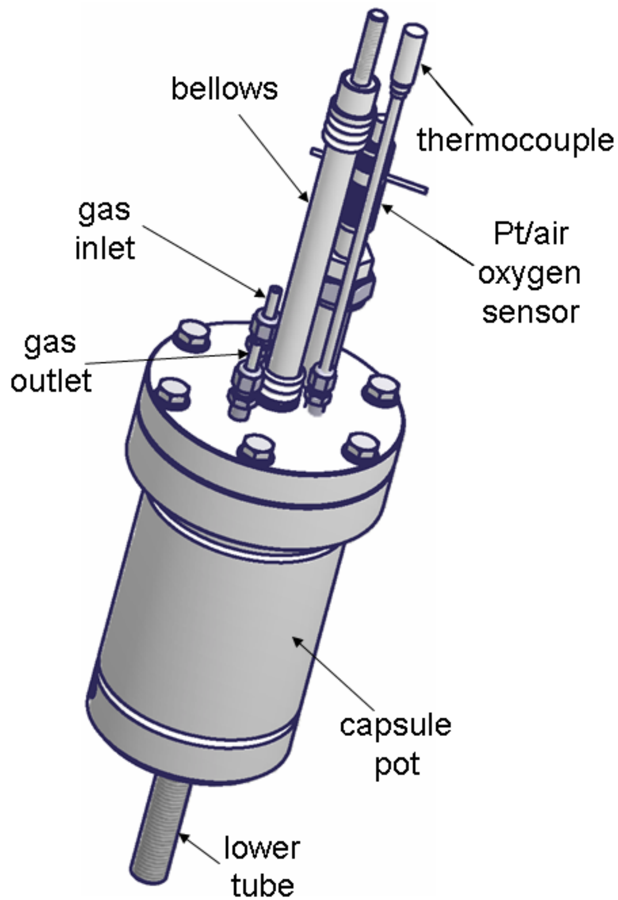


CRISLA- capsule main parts:

- Thermocouple
- Specimen holder
- Pt/air oxygen sensor
- Gas-inlet and -outlet
- Capsule: 316-Ti steel, internal coating with Al

# Operating efficiency of the new facility: pre-experiments in air at elevated temperature

## Tests in air at 650°C: two types of the specimens

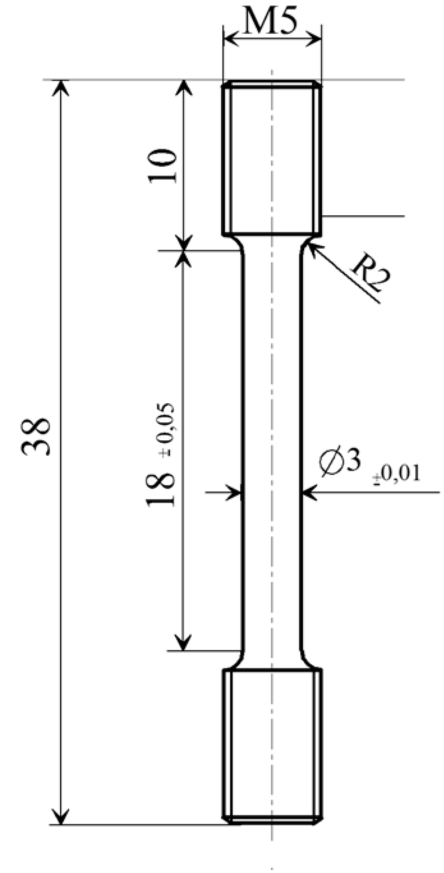


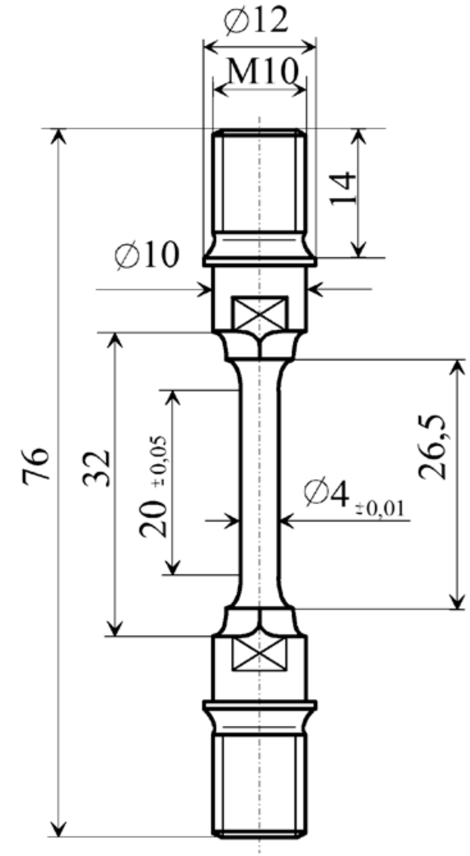

# CRISLA-Environment for Creep-Rupture Tests in Lead

## PC-supported control system for oxygen content: user defined settings

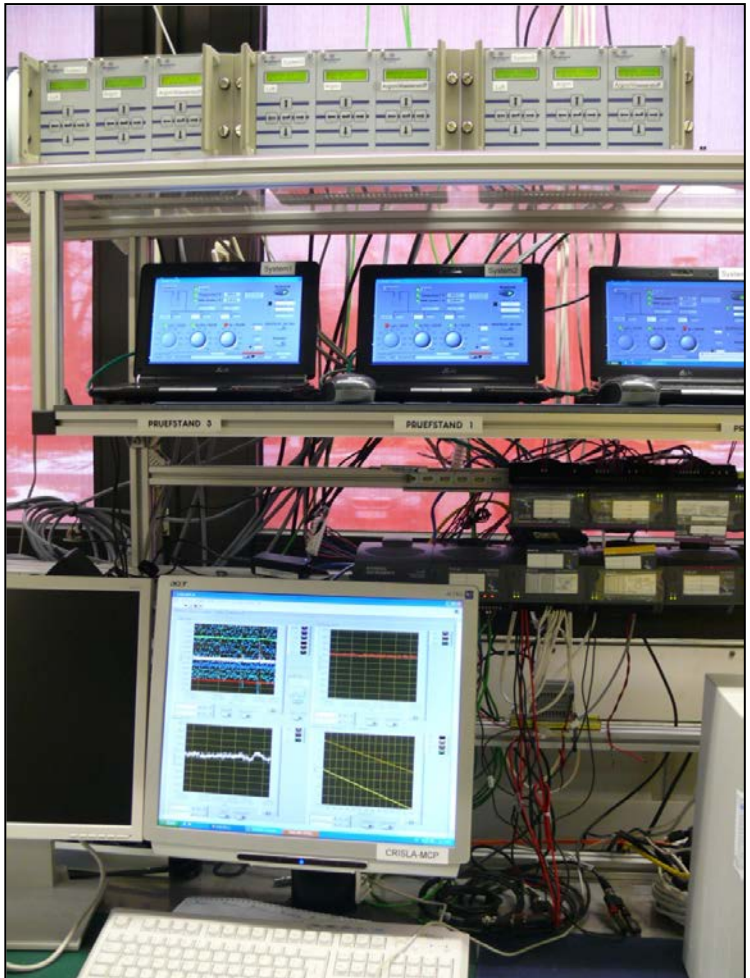


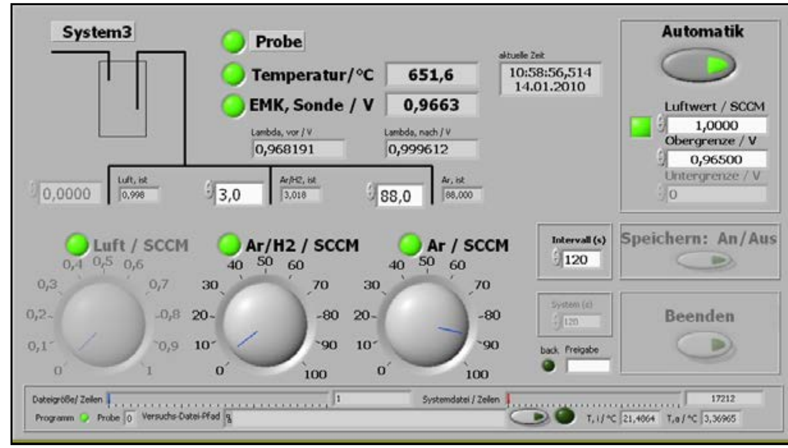


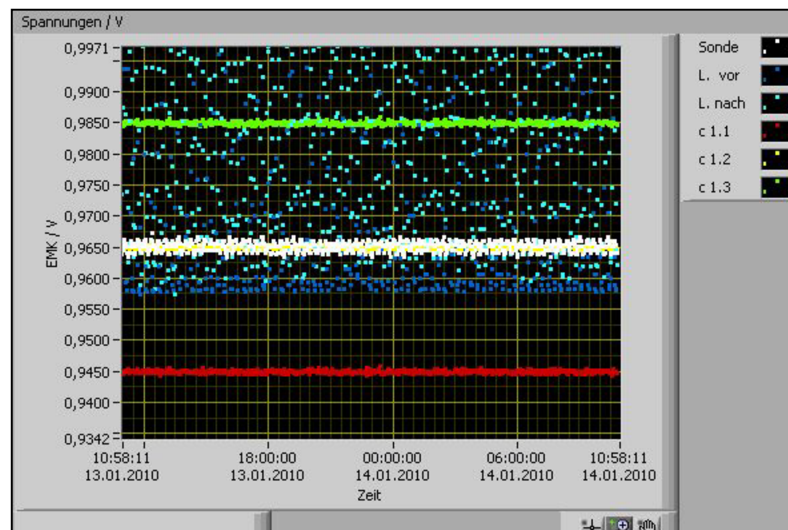

# Creep strength of T91 in air and lead at 650°C

Experimental and literature data for T91 in air

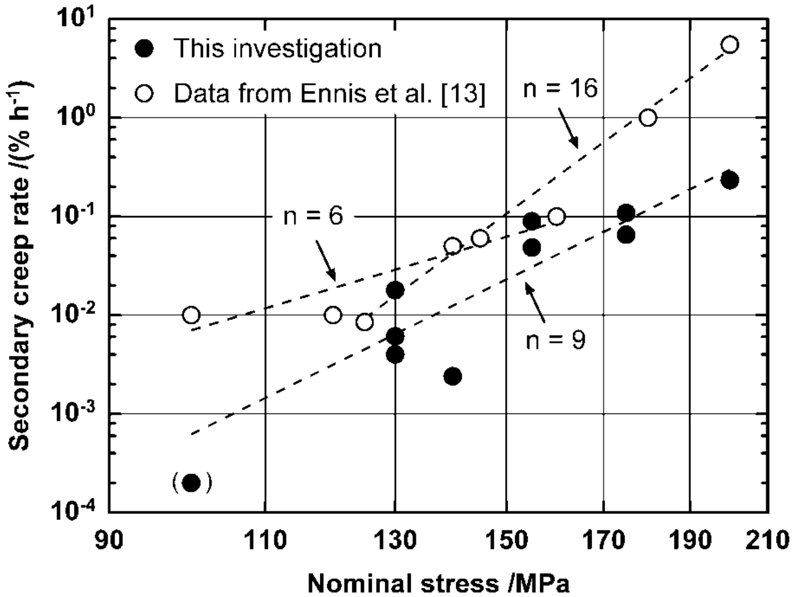


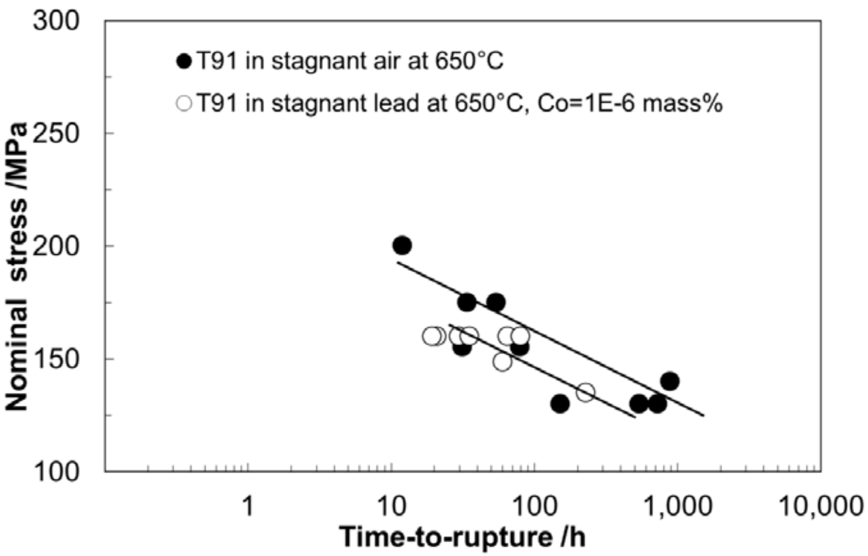


Stress exponent n in Northon law:

$$\dot{\varepsilon}_s = k\sigma^n$$

No great difference in creep strength of T91 tested in both environments

# Creep strength of P92 in air and lead at 650°C

Experimental and literature data for T91 in air

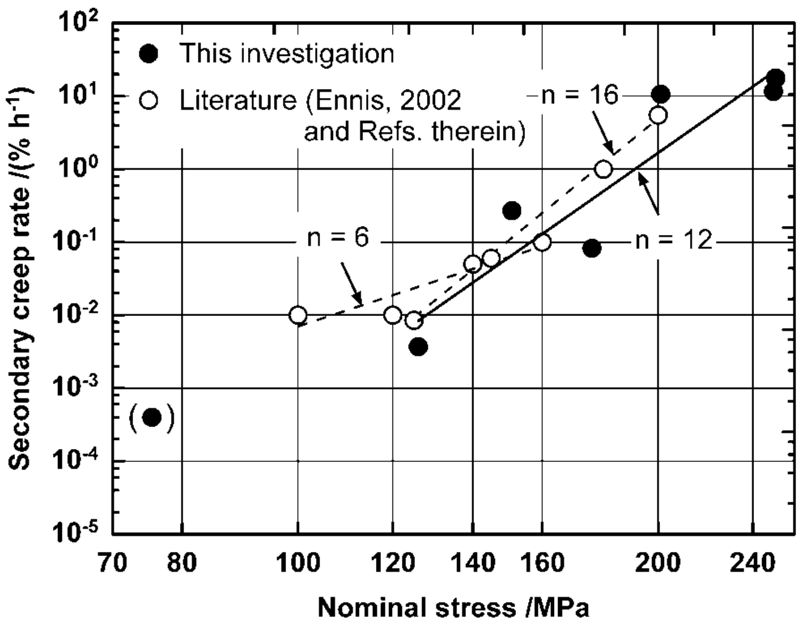


Stress exponent n in Northon law:

$$\dot{\varepsilon}_s = k\sigma^n$$

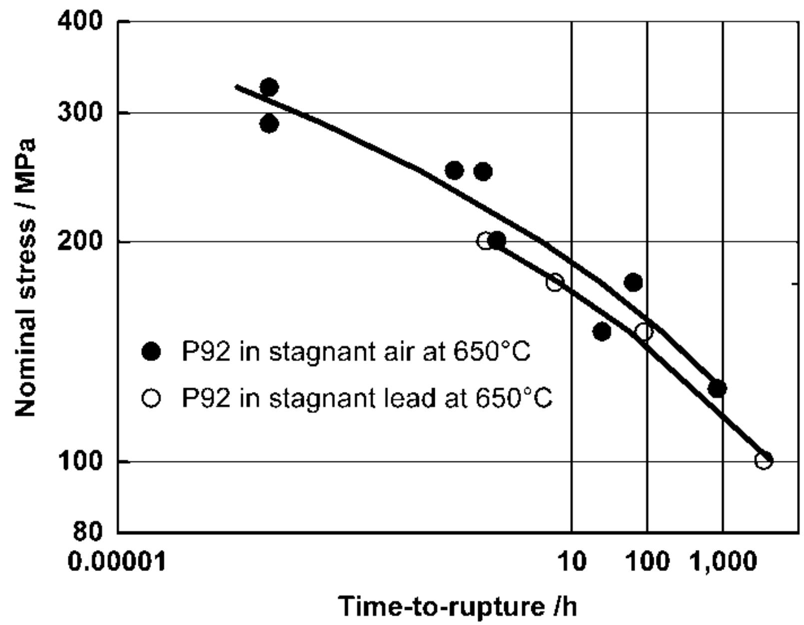


Creep strength exhibited in Pb is on the low scattering range limit of that obtained in air

# Creep strength of 14Cr-1W and 12Cr-2W ODS steels in stagnant lead ($c_o = 10^{-6}$ mass%) and air at 650°C

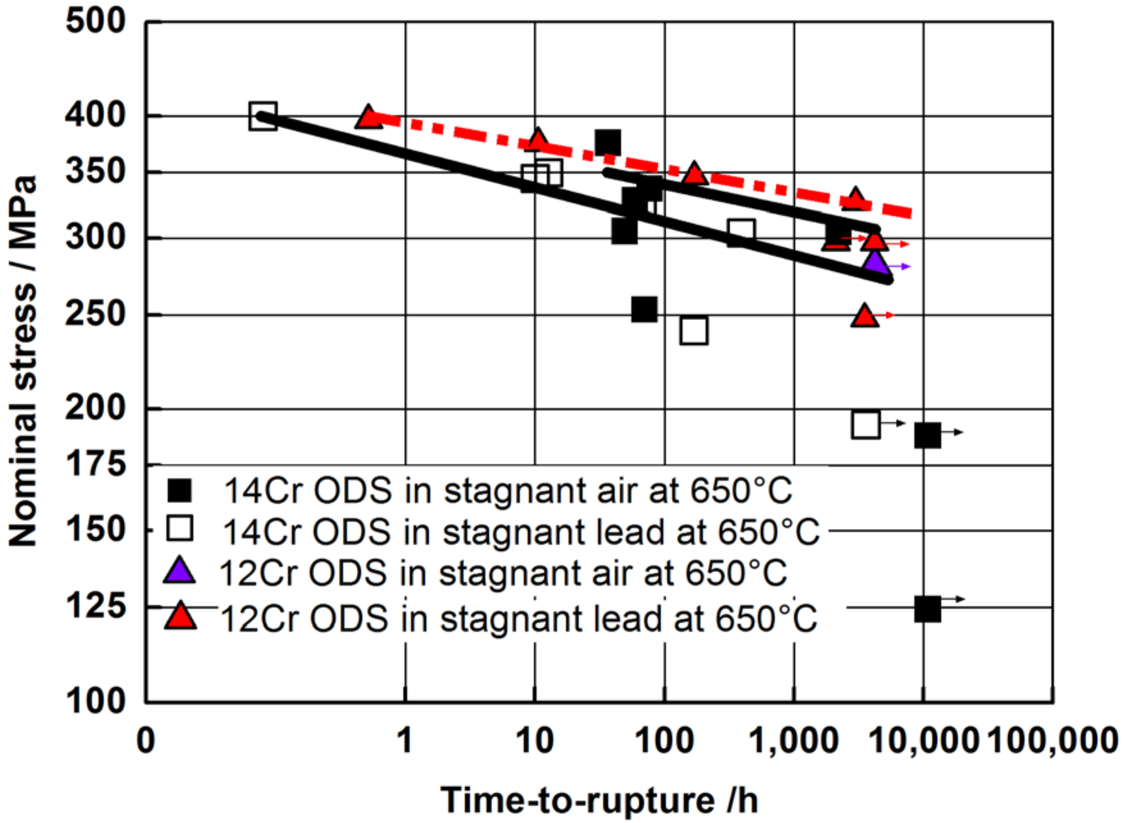


The 12-Cr ODS steel exhibits a slightly higher creep strength in stagnant Pb than the 14Cr-ODS steel

# Conclusions

- Heavy liquid metals (HLMs) are very appropriate coolants/targets for Nuclear (ADS, LFR) and Fusion (blanket) applications. Worldwide R&D has been established to buildup databases for compatibility issues of potential reference materials. A realization of first large demonstration plants within a time scale of about 25 years seems to be reasonable.
- The chemistry of materials corrosion issues in HLMs, i.e. the influence of oxygen as the major non-metal, is well characterized and understood.
- The accuracy of developed oxygen sensors, as part of required oxygen control systems, is reliable enough for evaluating the chemistry of HLMs. The feasibility on laboratory scale has been successfully proven.
- Further progress in the development of new materials with sufficient stable oxide layer formation for long-term operation and up-scaling of oxygen control processes is still required.

# Acknowledgements

With contributions from
Carsten Schroer, Wolfgang Krauss, Mariya Yurechko
and Olaf Wedemeyer

Funding by the EURATOM 6th Framework Programme
within the integrated project
(IP) EUROTRANS
(contract no. FI6W-CT-2004-516520)
is gratefully acknowledged.